University of Zurich[UZH]

Master Thesis

Sensitivity Analysis for Boundary Element Quadrature

Author:
Martino Antognini

Supervisor:
Prof. Dr. Stefan Sauter
Dr. Maria Lopez-Fernandez

25 Juli 2014

Contents

1 Introduction

In many scientific fields, a common problem is the computation of definite integrals of functions. For some integrals it is impossible to analytically compute their exact value. Instead, numerical methods like the Gaussian quadrature are used. The subject of this thesis is the Tensor-Gaussian quadrature applied to one particular problem, namely the three-dimensional wave equation.

An elegant procedure for solving partial differential equations like the wave equation is considered: The differential equation is transformed to an integral equation using an adequate ansatz; the integral equation is then transferred onto the Laplace domain by using the Laplace transform; and the problem is finally reduced to solving a coupled system of an integral equation on the boundary and a system of ordinary differential equations. Instead of solving the classical formulation of the integral equation, we use the variational formulation in order to apply a Galerkin method.

A demanding task for this procedure is the setup and solution process of a linear system of equations with a massive dense system matrix of dimension $\sim 10^4 - 10^5$. The entries of this matrix are integrals of the form

$$\int_\Gamma b_i(\mathbf{x}) \int_\Gamma k(\mathbf{x}, \mathbf{y}, \mathbf{x}-\mathbf{y}) b_j(\mathbf{y}) \, d\Gamma_y \, d\Gamma_x, \tag{1.1}$$

where the b_i are basis functions of the boundary element space, k is a kernel operator and Γ is the boundary of the integration domain.

Our goal is to analyze the behavior of the error of the Tensor-Gaussian quadrature applied to integrals such as (1.1). This error will depend on many parameters, such as the mesh size and the steps of the time discretization. The intent of our work is to experimentally study the influence of these parameters in order to optimize the performance of the method.

In Section 2, we formulate the problem. In Section 3, we introduce the numerical methods we use. Moreover, some theoretical frameworks are collected in the appendix. Section 4 is a brief summary of the theory about numerical integration and in particular about Gaussian quadrature in one and more dimensions. In Section 5, the concrete setup of the experiments is presented. Section 6 contains a small overview of the MATLAB implementation of the experiments. In particular, it also explains how the approximations could be reused for possible additional analyses. The results of the numerical experiments are then shown in Section 7. Finally, some conclusions are drawn in Section 8.

2 Formulation of the problem

The goal of this section is to briefly introduce the mathematical problem that we study. Part of the mathematical theory used in this section is presented in Appendix A. Additional theory can be found in e.g. [LFS12a, LFS12b], where the same problem is discussed with other goals.

2.1 The wave equation

Let $\Omega^- \subset \mathbb{R}^3$ be a bounded Lipschitz domain with boundary Γ. The unbounded complement is denoted by $\Omega^+ := \mathbb{R}^3 \backslash \overline{\Omega^-}$. Let $\Omega \in \{\Omega^-, \Omega^+\}$, and let $T > 0$ be a final time. Consider the homogeneous wave equation

$$\begin{aligned} \partial_t^2 U - \Delta U &= 0 && \text{in } \Omega \times (0,T) \\ U(\cdot,0) &= 0 && \text{in } \Omega \\ \partial_t U(\cdot,0) &= 0 && \text{in } \Omega \\ U &= g && \text{on } \Gamma \times (0,T), \end{aligned} \tag{2.1}$$

where $g : \Gamma \times (0,T) \to \mathbb{C}$ is a sufficiently smooth and compatible boundary condition.

2.2 Integral formulation

As in [Lub94], we employ as an ansatz the single-layer potential

$$U(x,t) = \int_0^t \int_\Gamma \frac{\delta(t - \tau - \|x-y\|)}{4\pi \|x-y\|} \phi(y,\tau)\, d\Gamma_y\, d\tau \quad \forall x \in \Omega, \forall 0 < t \le T, \tag{2.2}$$

where

$$\frac{\delta(t - \|x\|)}{4\pi \|x\|} \tag{2.3}$$

is the fundamental solution of the wave equation and δ is the Dirac delta distribution. This results in the following boundary integral equation for the density ϕ:

$$\int_0^t \big(k(t)\phi\big)(x,\tau)\, d\tau = g(x,t) \quad \forall t \in (0,T), x \in \Gamma, \tag{2.4}$$

where $k(t) : H^{-1/2}(\Gamma) \to H^{1/2}(\Gamma)$ is the kernel operator given by

$$\big(k(t)\phi\big)(x) = \int_\Gamma \frac{\delta(t - \|x-y\|)}{4\pi \|x-y\|} \phi(y)\, d\Gamma_y \quad \forall x \in \Gamma.$$

We refer to (2.4) as the *single-layer potential equation of the wave equation*. If g is sufficiently smooth and compatible, then this equation has a smooth solution. For proofs of existence and uniqueness of a solution, see [Lub94, BHD86].

The Sobolev spaces $H^s(\Gamma)$, $s \geq 0$, are defined in the usual way (cf. [Hac92]). The range of s for which $H^s(\Gamma)$ is defined may be limited depending on the global smoothness of the surface Γ. Throughout, we let $[-r, r]$ denote the range of Sobolev indices for which $H^s(\Gamma)$ is defined. The spaces of negative order are defined by duality in the usual way (cf [Hac92, Chapter 6.3]).

2.3 Problem on the Laplace domain

As in Section 3 of [LFS12a], we move to the Laplace domain by using the inverse Laplace transform of k. Therefore, let us first introduce the definition of the Laplace transform, which can be found e.g. in [EBY99].

Definition 1. Let $f: \mathbb{R} \to \mathbb{R}$ be a function with $f(t) = 0$ for $t < 0$. One says that f is *Laplace transformable* on the half-plane $\mathbb{C}_{>\sigma_0} = \{s \in \mathbb{C} \mid \mathrm{Re}(s) > \sigma_0\}$ if there exists a $\sigma_0 \in \mathbb{R}$ such that $e^{-\sigma_0 t} f(t)$ is integrable over $\mathbb{R}$. In this case, we call

$$(\mathcal{L}f)(s) = F(s) := \int_0^\infty f(t) e^{-st}\, dt.$$

the *Laplace transform* of f.

However, we are more interested in an inverse operator from $F(s)$ to $f(t)$.

Lemma 1. *Let f be Laplace transformable, let σ_0 as in Definition 1 and let $F(s) = (\mathcal{L}f)(s)$ be its Laplace transform. The inverse Laplace transform is given by*

$$f(t) = (\mathcal{L}^{-1}F)(t) := \frac{1}{2\pi \mathrm{i}} \int_{\sigma + \mathrm{i}\mathbb{R}} F(s) e^{st}\, ds$$

for $t \in \mathbb{R}$, $\sigma > \sigma_0$.

The theory for the Laplace transform can be extended to distribution (cf. e.g. [Jan71]).

The Laplace transform of the fundamental solution to the wave equation

$$\frac{\delta(t - \|x\|)}{4\pi \|x\|}$$

with respect to t gives

$$K(x, s) = \frac{e^{-s\|x\|}}{4\pi \|x\|}. \tag{2.5}$$

We can now write the left-hand side of (2.4) as

$$\begin{aligned}
\int_0^t \big(k(t)\phi\big)(x, \tau)\, d\tau &= \int_0^t \int_\Gamma k(x - y, t - \tau) \phi(y, \tau)\, d\Gamma_y d\tau \\
&= \int_0^t \int_\Gamma \frac{1}{2\pi \mathrm{i}} \int_\gamma e^{z(t-\tau)} K(x - y, z)\, dz\, \phi(y, \tau)\, d\Gamma_y d\tau \\
&= \frac{1}{2\pi \mathrm{i}} \int_0^t \int_\gamma e^{z(t-\tau)} \big(\mathcal{K}(z)\phi\big)(x)\, dz\, d\tau,
\end{aligned}$$

where $\gamma = \sigma_0 + \mathrm{i}\mathbb{R}$ for some $\sigma_0 > 0$ and $\mathcal{K}(z)\psi$ is the Laplace transformed integral operator, i.e. the transfer operator for $k_\psi(t)$ given by

$$\big(\mathcal{K}(z)\psi\big)(x) := \int_\Gamma K(x-y,z)\psi(y)d\Gamma_y. \tag{2.6}$$

We thus rewrite (2.4) by exchanging the order of the integrals and obtain

$$\frac{1}{2\pi\mathrm{i}}\int_\gamma \mathcal{K}(z)\int_0^t e^{z(t-\tau)}\phi(\,\cdot\,,\tau)\,d\tau\,dz = g(x,t). \tag{2.7}$$

Note that $\int_0^t e^{z(t-\tau)}\phi(y,\tau)\,d\tau =: u(y,z,t)$ solves the ordinary differential equation

$$\begin{aligned}\partial_t u(\,\cdot\,,z,t) &= zu(\,\cdot\,,z,t) + \phi(\,\cdot\,,t)\\ u(\,\cdot\,,z,0) &= 0,\end{aligned}$$

so (2.4) can be reduced to solving the coupled system of an ordinary differential equation and an integral equation

$$\begin{aligned}\frac{1}{2\pi\mathrm{i}}\int_\gamma \mathcal{K}(z)u(z,t)\,dz &= g(t)\\ \partial_t u(z,t) &= zu(z,t) + \phi(t)\\ u(z,0) &= 0\end{aligned} \tag{2.8}$$

for $\phi\colon[0,T] \to H^{-1/2}(\Gamma)$ and $u\colon\gamma\times[0,T] \to H^{-1/2}(\Gamma)$. Note that the integral equation must hold for all $x \in \Gamma$. For simplicity, we omit the argument on both sides of the equation.

3 Numerical methods

To find a solution of the wave equation (2.1), one has to solve the coupled system (2.8)

$$\begin{aligned}\frac{1}{2\pi \mathrm{i}} \int_\gamma \mathcal{K}(z) u(z,t)\, dz &= g(t) \\ \partial_t u(z,t) &= z u(z,t) + \phi(t) \\ u(z,0) &= 0.\end{aligned}$$

In this section we present the numerical methods used to solve this problem. We first employ discretizations in time and space, and then a quadrature for the complex contour integral.

3.1 Temporal discretization

We consider the discretization in time used in [LFS12a] and [LFS12b]. For this, let

$$0 = t_0 < t_1 < \cdots < t_N = T,$$

be the points in time at which we want to discretize. We define the steps

$$\begin{aligned}\Delta_j &:= t_j - t_{j-1} \qquad \text{for } 1 \le j \le N \\ \Delta &:= \max_{1 \le j \le N} \Delta_j.\end{aligned} \tag{3.1}$$

We denote by $u_j(z) \in H^{-1/2}(\Gamma)$ and $\phi_j \in H^{-1/2}(\Gamma)$ the approximation of $u(z,t_j)$ and $\phi(t_j)$ at time $t_j, 0 \le j \le N$ respectively.

The initial values $u_0(z) = 0$ and $\phi_0 = 0$ are given. Let us assume that we know the approximate values $u_\ell(z)$ and ϕ_ℓ for $1 \le \ell \le j$. Our goal is to compute $u_{j+1}(z)$ and ϕ_{j+1}. We apply the implicit Euler method to the ordinary differential equation of the coupled system (2.8) and get

$$u_{j+1}(z) = \frac{1}{1 - z\Delta_{j+1}} u_j(z) + \frac{\Delta_{j+1}}{1 - z\Delta_{j+1}} \phi_{j+1}. \tag{3.2}$$

This expression is then inserted in the integral equation

$$\frac{1}{2\pi \mathrm{i}} \int_\gamma \mathcal{K}(z) u_{j+1}(z)\, dz = g_{j+1}$$

of (2.8), giving

$$\frac{1}{2\pi \mathrm{i}} \int_\gamma \frac{\mathcal{K}(z)}{1 - z\Delta_{j+1}} u_j(z)\, dz + \frac{1}{2\pi \mathrm{i}} \int_\gamma \frac{\mathcal{K}(z)}{\frac{1}{\Delta_{j+1}} - z} \phi_{j+1}\, dz = g_{j+1}.$$

Note that the only unknown is ϕ_{j+1}. We now apply Cauchy's integral formula to the left-hand side. For this, we require that $0 < \sigma_0 < \frac{1}{\Delta}$ in the contour $\gamma = \sigma_0 + \mathrm{i}\mathbb{R}$. We obtain

$$\mathcal{K}\left(\frac{1}{\Delta_{j+1}}\right)\phi_{j+1} = g_{j+1} - \frac{1}{2\pi\mathrm{i}}\int_\gamma \frac{\mathcal{K}(z)}{1 - z\Delta_{j+1}} u_j(z)\,dz. \tag{3.3}$$

One has to solve (3.3) for ϕ_{j+1} and then insert the result into (3.2) to get $u_{j+1}(z)$ for the next step.

3.2 Boundary element spaces

We now define an appropriate finite dimensional subspace of our function space $H^s(\Gamma)$ in order to perform a Galerkin discretization (see Subsection A.3). We triangulate the boundary Γ, following [SS11, Chapter 4.1.2]. We will restrict ourselves to plane triangles with straight edges, i.e. Γ is the surface of a polyhedron.

We first define the *reference triangle* $\hat{\tau}$

$$\hat{\tau} := \left\{ \begin{pmatrix} x_1 \\ x_2 \end{pmatrix} \in \mathbb{R}^2 \;\middle|\; 0 \le x_2 \le x_1 \le 1 \right\} = \operatorname{conv}\left\{ \begin{pmatrix} 0 \\ 0 \end{pmatrix}, \begin{pmatrix} 1 \\ 0 \end{pmatrix}, \begin{pmatrix} 0 \\ 1 \end{pmatrix} \right\} \subset \mathbb{R}^2.$$

For any triangle τ with vertices $\mathbf{A} = (a_1, a_2, a_3), \mathbf{B} = (b_1, b_2, b_3), \mathbf{C} = (c_1, c_2, c_3) \in \mathbb{R}^3$ we can now define the matrix

$$\mathbf{M}_\tau := \begin{pmatrix} b_1 - a_1 & c_1 - b_1 \\ b_2 - a_2 & c_2 - b_2 \\ b_3 - a_3 & c_3 - b_3 \end{pmatrix} = \Big(\mathbf{B} - \mathbf{A}\Big|\mathbf{C} - \mathbf{B}\Big), \tag{3.4}$$

and the affine parametrization

$$\begin{aligned} \chi_\tau : \hat{\tau} &\to \tau \\ \hat{\mathbf{x}} &\mapsto \mathbf{A} + \mathbf{M}_\tau \hat{\mathbf{x}}, \end{aligned} \tag{3.5}$$

whose Jacobian is $\mathbf{M}_\tau$.

Definition 2. A *paneling* $\mathcal{G}$ of the boundary Γ is a partitioning of Γ into finitely many closed triangles $\tau \subset \Gamma$, that satisfies:

(i) $\mathcal{G}$ covers Γ:

$$\Gamma = \overline{\bigcup_{\tau \in \mathcal{G}} \tau}$$

(ii) Every triangle $\tau \in \mathcal{G}$ is the image of an affine parametrization $\chi_\tau : \hat{\tau} \to \tau$ as described in (3.5).

(iii) If the triangles are non-degenerate (i.e. the vertices are not collinear), there exist $\lambda_{\min}, \lambda_{\max} > 0$ such that

$$0 < \lambda_{\min} \leq \inf_{v \in \mathbb{R}^2, \|v\|=1} v^T \mathbf{M}_\tau^T \mathbf{M}_\tau v \leq \sup_{v \in \mathbb{R}^2, \|v\|=1} v^T \mathbf{M}_\tau^T \mathbf{M}_\tau v \leq \lambda_{\max} < \infty. \quad (3.6)$$

If this is the case, χ_τ is called *regular*.

Definition 3. A paneling $\mathcal{G}$ is called *regular*, if

(i) For any two distinct triangles $\tau, \tau_* \in \mathcal{G}$, their intersection is either empty or consists only of a common edge or vertex.

(ii) If $\tau, \tau_* \in \mathcal{G}$, intersect in a common edge $e = \overline{\tau} \cap \overline{\tau_*}$, then their parametrizations are compatible, i.e.

$$\chi_\tau|_{\hat{e}} = \chi_{\tau_*} \circ \gamma_{\tau,\tau_*}|_{\hat{e}},$$

where $\hat{e} = \chi_\tau^{-1}(e)$ and $\gamma_{\tau,\tau_*} : \hat{\tau} \to \hat{\tau}$ is an affine bijection.

Note that in practice our domain Ω will usually not be polyhedral. If Γ is curved, then an additional error arises. For an analysis of this error see [SS11].

Let us now define some attributes of the paneling.

Definition 4. Let $\mathcal{G}$ be a regular paneling.

(i) The diameter of a triangle $\tau \in \mathcal{G}$ is $h_\tau := \max_{x,y \in \tau} \|x - y\|$.

(ii) The inner width ρ_τ of τ is its incircle diameter.

(iii) The paneling width of $\mathcal{G}$ is $h_\mathcal{G} := \max_{\tau \in \mathcal{G}} h_\tau$.

(iv) The shape-regularity constant of $\mathcal{G}$ is $\kappa_\mathcal{G} := \max_{\tau \in \mathcal{G}} (h_\tau / \rho_\tau)$.

(v) The quasi-uniformity constant of $\mathcal{G}$ is $q_\mathcal{G} := h_\mathcal{G} / (\min_{\tau \in \mathcal{G}} h_\tau)$.

(vi) The number of triangles of $\mathcal{G}$ is $n_T = |\mathcal{G}|$.

We will now give the definition of the boundary element space. In our numerical experiments, we only take into account piecewise constant boundary elements. An extension of the code to piecewise linear boundary elements should be easy to implement.

Let Γ be a polygonal boundary and $\mathcal{G}$ a paneling of it. We then define

$$S_\mathcal{G}^0 := \{u \in L^\infty(\Gamma) \mid \forall \tau \in \mathcal{G} : u|_\tau \circ \chi_\tau \in \mathbb{P}_0\}, \quad (3.7)$$

where $\mathbb{P}_0$ is the space of all constant functions on $\hat{\tau}$. Notice that $S_\mathcal{G}^0 \subset H^{-1/2}(\Gamma)$.

We can easily define a basis $(b_k^{\mathcal{G},0})_{k=1,\dots,M}$ of $S_\mathcal{G}^0$ given by

$$b_k^{\mathcal{G},0}(x) = \begin{cases} 1 & x \in \tau_k \\ 0 & \text{else,} \end{cases} \quad (3.8)$$

where the triangles of $\mathcal{G}$ are numbered $\tau_1, \ldots, \tau_{n_T}$. Hence, the dimension of $S^0_{\mathcal{G}}$ is $M := n_T$. For spaces $S^p_{\mathcal{G}}$ of order $p > 0$, consult [SS11, Chapter 4.1.2, 4.1.7].

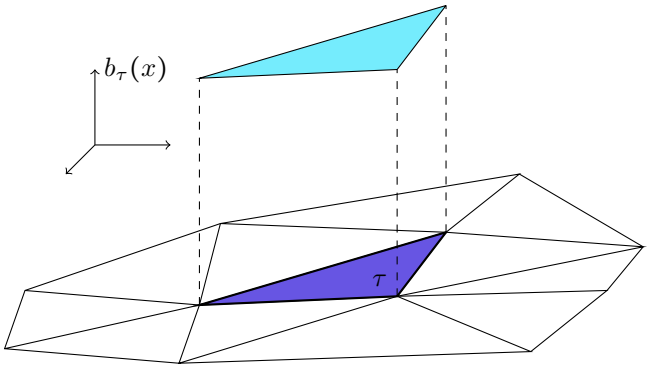

Figure 3.1: Piecewise constant basis function b_τ, as defined in (3.8).

3.3 Spatial discretization

Let $\mathcal{G}_j$ be the mesh approximating Γ at time step[1] t_j, $0 \le j \le N$ as presented in Subsection 3.2. We denote by M_j the dimension of $S^0_{\mathcal{G}_j}$ and by b^j_k the bases $b^{\mathcal{G}_j,0}_k, 1 \le k \le M_j$.

The Galerkin discretization of (3.3) is then given by

Find $\phi_{j+1} \in S^0_{\mathcal{G}_{j+1}}$ such that

$$\left(\mathcal{K}\left(\frac{1}{\Delta_{j+1}}\right)\phi_{j+1}, v\right)_{L^2(\Gamma)} = (g_{j+1}, v)_{L^2(\Gamma)} - \left(\frac{1}{2\pi \mathrm{i}}\int_\gamma \frac{\mathcal{K}(z)u_j(z)}{1 - z\Delta_{j+1}}\,dz, v\right)_{L^2(\Gamma)} \quad \forall v \in S^0_{\mathcal{G}_{j+1}}. \tag{3.9}$$

The elements of $S^0_{\mathcal{G}_{j+1}}$, ϕ_{j+1} and $u_{j+1}(z)$ can be written as

$$\phi_{j+1} = \sum_{\ell=1}^{M_j} (\boldsymbol{\phi}_{j+1})_\ell b^{j+1,p}_\ell,$$
$$u_{j+1}(z) = \sum_{\ell=1}^{M_j} (\mathbf{u}_{j+1}(z))_\ell b^{j+1,p}_\ell.$$

Furthermore, we define the Helmholtz matrices

$$(\mathbf{K}_{j+1}(z))_{k,\ell} := (\mathcal{K}(z)b^{j+1}_\ell, b^{j+1}_k)_{L^2(\Gamma)} \tag{3.10}$$

[1] The mesh $\mathcal{G}$ can be adapted after each time step, see [Sch12].

and the right-hand side vector

$$(\mathbf{g}_{j+1})_k \coloneqq (g_{j+1}, b_k^{j+1})_{L^2(\Gamma)}. \tag{3.11}$$

Let us denote by $\mathbf{P}_j \colon S^p_{\mathcal{G}_j} \to S^p_{\mathcal{G}_{j+1}}$ the prolongation from one mesh to the next in matrix representation. We can now rewrite (3.3) and (3.2) as follows:

$$\mathbf{K}_{j+1}\left(\frac{1}{\Delta_{j+1}}\right)\boldsymbol{\phi}_{j+1} = \mathbf{g}_{j+1} - \frac{1}{2\pi \mathrm{i}}\int_\gamma \frac{\mathbf{K}_{j+1}(z)\mathbf{P}_j\mathbf{u}_j(z)}{1 - z\Delta_{j+1}}\,dz \tag{3.12}$$

$$\mathbf{u}_{j+1}(z) = \frac{1}{1 - z\Delta_{j+1}}\mathbf{P}_j\mathbf{u}_j(z) + \frac{\Delta_{j+1}}{1 - z\Delta_{j+1}}\boldsymbol{\phi}_{j+1}. \tag{3.13}$$

3.4 Contour quadrature

We now have to resolve the contour integral

$$\int_\gamma \frac{\mathbf{K}_{j+1}(z)\mathbf{P}_j\mathbf{u}_j(z)}{1 - z\Delta_{j+1}}\,dz. \tag{3.14}$$

For this, an appropriate quadrature technique should be used. By the Cauchy theorem, we can replace the contour $\gamma = \sigma_0 + \mathrm{i}\mathbb{R}$ by any negatively oriented contour in the positive complex plane that surrounds the poles $\frac{1}{\Delta_j}$, $1 \le j \le N$. For this, we define

$$m = \frac{1}{\Delta}, \tag{3.15}$$

$$M = \max\left(\left\{m^2\right\} \cup \left\{ \frac{1}{\Delta_j} \;\middle|\; 1 \le j \le N \right\}\right), \tag{3.16}$$

$$q = \frac{M}{m}, \tag{3.17}$$

where Δ and Δ_j are as in (3.1). For simplicity we will assume that $m \ge 2$.
We consider the circle centered at M with radius M, following the implementation proposed in [LFS12b].

4 Numerical integration

In this section we introduce the concept of numerical integration and in particular of Gaussian quadrature, first in one and then in multiple dimensions. Moreover, we will present a derivative-free error estimation.

4.1 Introduction

We start by introducing the notion of quadrature for the one-dimensional case. Given a function $f \in C^0(J)$ for an interval $J = [a, b] \subset \mathbb{R}$, we want to approximate the value of the definite integral

$$\mathcal{I}_J(f) \coloneqq \int_J f(x)w(x)\,dx, \tag{4.1}$$

where $w : J \to \mathbb{R}$ is a positive weight function. The Gaussian quadrature belongs to the family of quadrature rules based on interpolation. The procedure consists of dividing the integration domain J into subintervals and interpolating the integrand on these subintervals by polynomials, which can be integrated exactly.

A quadrature of order n is therefore

$$\mathcal{I}_J(f) \approx \sum_{i=1}^{n} \omega_i f(x_i) =: Q_{n,J}(f), \tag{4.2}$$

where the x_i are called *nodes* and the ω_i are called *weights* of the quadrature formula. The values of the weights depend on the choice of the nodes and the order of the interpolation. The error of the quadrature is denoted by

$$\mathcal{E}_{n,J}(f) \coloneqq \mathcal{I}_J(f) - Q_{n,J}(f). \tag{4.3}$$

For simplicity, we let $\mathcal{I} = \mathcal{I}_J$, $Q_n = Q_{n,J}$, $\mathcal{E}_n = \mathcal{E}_{n,J}$. We denote by $\mathbb{P}_k$ the set of all real polynomials of degree at most k:

$$\mathbb{P}_k \coloneqq \{a_0 + a_1 x + \ldots + a_k x^k \mid a_i \in \mathbb{R} \forall 0 \le i \le k\}. \tag{4.4}$$

Definition 5. A quadrature rule has *degree of exactness* k, if

$$\mathcal{E}_n(p) = 0 \qquad \forall p \in \mathbb{P}_k, J \subset \mathbb{R},$$

and there exists at least one $p_* \in \mathbb{P}_{k+1}$ such that $\mathcal{E}_n(p_*) \neq 0$.

Note that if a quadrature rule based on polynomial interpolation, then the value of the integral is computed exactly for every polynomial of degree $\le n$, and so the degree of exactness k is always $\ge n$.

Definition 6. A quadrature is called *stable* if

$$\sum_{i=1}^{n} \omega_i = |J|$$

and there exists a $C_Q \in \mathbb{R}$ such that

$$\sum_{i=1}^{n} |\omega_i| \leq C_Q \sum_{i=1}^{n} \omega_i.$$

The constant C_Q is called the *stability constant* of the quadrature.

It is convenient[2] to scale the domain of integration to a reference interval $\widehat{J} = [-1, 1]$. For this, we define the parametrization

$$\begin{aligned} \chi\colon \widehat{J} &\to J \\ \hat{x} &\mapsto \chi(\hat{x}) = \frac{a+b}{2} + \hat{x}\frac{b-a}{2}, \end{aligned} \tag{4.5}$$

and its inverse

$$\begin{aligned} \chi^{-1}\colon J &\to \widehat{J} \\ x &\mapsto \chi^{-1}(x) = \frac{2}{b-a}x - \frac{a+b}{b-a}. \end{aligned} \tag{4.6}$$

We can now rewrite (4.1) as

$$\mathcal{I}_J(f) = \int_J f(x)w(x)\,dx = \int_{\widehat{J}} f(\chi(\hat{x}))w(\chi(\hat{x}))\chi'(\hat{x})\,d\hat{x}. \tag{4.7}$$

4.2 One-dimensional Gaussian quadrature

For a function $f \in C^0(J)$ and a set of nodes $\mathcal{G}_n := \{\xi_i \mid 1 \leq i \leq n\} \subset J$, the interpolation polynomial $p_n(f, \mathcal{G}_n)$ is unique. We write it in the Lagrange-representation

$$f(x) \approx p_n(f, \mathcal{G}_n)(x) := \sum_{i=1}^{n} f(\xi_i) l_i(x), \tag{4.8}$$

where

$$l_i(x) = \prod_{\substack{j=1 \\ j \neq i}}^{n} \frac{x - \xi_j}{\xi_i - \xi_j}. \tag{4.9}$$

We insert the interpolation polynomial in (4.2) and obtain

$$Q_n(f) = \int_J p_n(f, \mathcal{G}_n)(x)w(x)\,dx = \sum_{i=1}^{n} f(\xi_i)\omega_i, \tag{4.10}$$

[2] In the numerical experiment in Chapter 5, we will compute many integrals on different domains. For this, it is worthwhile to scale the domains and to compute the Gaussian nodes and weights on the reference domain once for all.

where the weights of the quadrature are defined by

$$\omega_i = \int_J l_i(x) w(x)\, dx \qquad \forall 1 \le i \le n. \tag{4.11}$$

The goal now is to find the highest degree of exactness. For this, we employ a theorem, whose proof can be found e.g. in [Sau10].

Theorem 2. *Let $d \in \mathbb{N}$. The quadrature formula (4.2) has degree of exactness $k = n + d$ if and only if the following conditions are fulfilled:*

(i) The quadrature (4.2) is based on interpolation.

(ii) The polynomial $s(x) := (x - \xi_1)\cdots(x - \xi_n)$ satisfies

$$\int_J s(x) p(x) w(x)\, dx = 0, \qquad \forall p \in \mathbb{P}_n. \tag{4.12}$$

Note that (ii) is a condition on the nodes ξ_i. Furthermore, for $w(x) > 0, w \in L^\infty(J)$,

$$\int_J u(x) v(x) w(x)\, dx =: a(u, v), \qquad u, v \in L^2(J), \tag{4.13}$$

defines a scalar product on $L^2(J)$. One says that two functions u, v are orthogonal with respect to $a(\cdot,\cdot)$ if $a(u, v) = 0$. Thus, condition (ii) means that $s(x)$ is orthogonal to every $p \in \mathbb{P}_d$. This implies[3] that $s(x) \notin \mathbb{P}_n$, and consequently $n > d$. Hence, the highest degree of exactness for a quadrature formula of order n is $k = 2n - 1$ ($d = n - 1$). Such quadratures are called Gaussian quadratures.

For the actual computation of the Gaussian nodes and weights, we will use polynomials p_j defined by the following recursion:

$$\begin{aligned} p_{-1}(x) &\equiv 0, \\ p_0(x) &\equiv 1, \\ p_{j+1}(x) &\equiv (x - \alpha_j) p_j(x) - \beta_j p_{j-1}(x), \qquad j \ge 0, \end{aligned}$$

where, with the scalar product defined in (4.13),

$$\begin{aligned} \alpha_j &= \frac{a(x p_j, p_j)}{a(p_j, p_j)}, \qquad j \ge 0, \\ \beta_j &= \frac{a(p_j, p_j)}{a(p_{j-1}, p_{j-1})}, \qquad j \ge 1, \\ \beta_0 &= \int_J w(x)\, dx = 1. \end{aligned}$$

By construction, we have

$$a(p_i, p_j) = \int_J p_i(x) p_j(x) w(x)\, dx = 0, \qquad \text{for } i \ne j. \tag{4.14}$$

[3] $s(x) \in \mathbb{P}_n$ implies $a(s, s) = 0$, but since $s \ne 0$, $a(s, s) > 0$

Since every polynom $p \in \mathbb{P}_k$ can be written as a linear combination of the p_j, $0 \le j \le k$, the generalization of (4.14) is:

$$a(p, p_k) = \int_J p(x) p_k(x) w(x)\, dx = 0, \qquad \forall p \in \mathbb{P}_{k-1}. \tag{4.15}$$

The nodes ξ_i, $1 \le i \le n$, of the Gaussian quadrature of order n are the roots of the polynomial p_n. The weights ω_i are the solutions to the system of linear equations

$$\begin{aligned} \sum_{i=1}^{n} \omega_i p_0(\xi_i) &= a(p_0, p_0) \\ \sum_{i=1}^{n} \omega_i p_j(\xi_i) &= 0, \qquad \forall 1 \le j \le n-1. \end{aligned}$$

It is easy to show that the Gaussian weights are all positive and that the Gaussian quadrature is stable.

We can now present a result about the error of the one-dimensional Gaussian quadrature from [Sto07].

Theorem 3. *For a sufficient smooth function $f \in C^{2n}(J)$ and a $\xi \in J$ we have*

$$\mathcal{E}_n(f) = \frac{f^{(2n)}(\xi)}{(2n)!} \int_J p_n(x)^2\, dx. \tag{4.16}$$

A proof of the theorem can be found in [Sto07]. Note that the error estimation strongly depends on the derivatives of the integrand. Therefore, it can be troublesome (or even impossible) to determine the order n of the quadrature for a given desired accuracy ϵ.

Theorem 4. *Let $f \in C(J)$. Then*

$$\lim_{n \to \infty} \mathcal{E}_n(f) = 0. \tag{4.17}$$

Proof. First recall that by the Weierstrass theorem, for every $\varepsilon_* > 0$, there exists a polynomial p such that $\|f - q\|_\infty < \varepsilon_*$. Let $m = \deg q$. We have

$$\begin{aligned} \mathcal{E}_n(f) &= \mathcal{I}(f) - Q_n(f) \\ &= \mathcal{I}(f) - \int_J q(x)\, dx + \int_J q(x)\, dx - Q_n(q) + Q_n(q) - Q_n(f). \end{aligned} \tag{4.18}$$

For the first two terms, we have

$$\left| \mathcal{I}(f) - \int_J q(x)\, dx \right| = \left| \int_J (f(x) - q(x))\, dx \right| \le \int_J |f(x) - q(x)|\, dx \le \varepsilon_* |J|. \tag{4.19}$$

Moreover, because of the degree of exactness of the quadrature, we have for every $n \ge (m-1)/2$

$$\int_J q(x)\, dx - Q_n(q) = 0. \tag{4.20}$$

Finally,

$$\begin{aligned}\left|Q_n(q) - Q_n(f)\right| &= \left|\sum_{i=1}^{n} \omega_i (q(\xi_i) - f(\xi_i))\right| \\ &\leq \sum_{i=1}^{n} |\omega_i|\,|(q(\xi_i) - f(\xi_i))| \leq \varepsilon_* \sum_{i=1}^{n} |\omega_i| \leq \varepsilon_* |J|,\end{aligned} \tag{4.21}$$

since all of the Gaussian weights are positive. The combination of (4.19), (4.20) and (4.21) in (4.18) gives us

$$\left|\mathcal{E}_{n,J}(f)\right| \leq 2\varepsilon_* \,|J|\,. \tag{4.22}$$

In particular, for the reference domain $\widehat{J} = [-1, 1]$, we have $|\mathcal{E}_{n,\widehat{J}}(f)| < 4\varepsilon_*$. This means that for an arbitrary $\varepsilon > 0$, we set $\varepsilon_* = \frac{\varepsilon}{2|J|}$ and obtain

$$\left|\mathcal{E}_{n,J}(f)\right| \leq \varepsilon \tag{4.23}$$

for sufficiently large n. Hence, the theorem holds. □

In Section 5 we will see that the functions we have to integrate are analytic. However, they have poles near the integration domain (more precisely in a complex neighbourhood). The kernel functions and their derivatives in local coordinates are in practice very difficult to estimate. Therefore, a derivative-free error estimation[4] is more convenient. We present hence a theorem from [SS11, Section 5.3.2.2].

We denote by $\Xi^{\rho}_{a,b} \subset \mathbb{C}$ the closed ellipse with focal points $a, b \in \mathbb{R}$, major semiaxis $\overline{a} > \frac{b-a}{2}$ and minor semiaxis $\overline{b} > 0$. $\rho = \overline{a} + \overline{b}$ is the sum of the two semiaxes. Since in practice we are only interested in the case $a = 0$ and $b = 1$, we abbreviate $\Xi^{\rho}_{0,1}$ by Ξ^{ρ}.

[4] With the expression "derivative-free error estimation" we mean an error estimation which does not depend on the derivative of the integrand, unlike in (4.16).

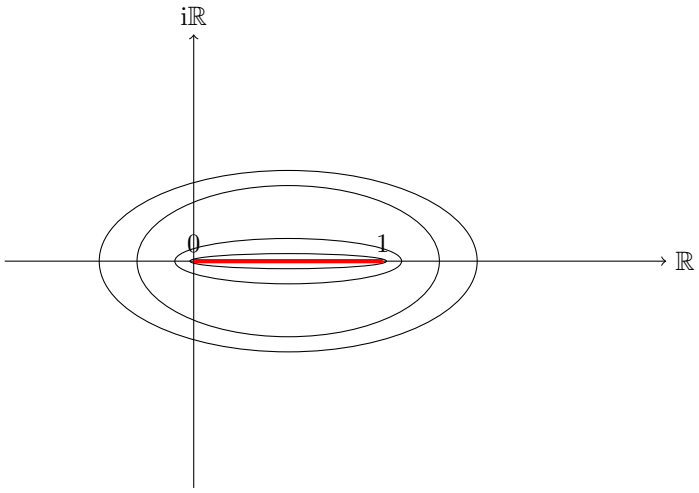

Figure 4.1: Ellipse $\Xi^{\rho}_{0,1}$ with focal points 0 and 1 on the real axis and semi-axes sum $\rho \in \{0.56, 0.72, 1.2, 1.88\}$.

Theorem 5. *Let $f\colon [0,1] \to \mathbb{C}$ be an analytic function with analytic continuation f^* on the ellipse $\Xi^{\rho} \subset \mathbb{C}, \rho > \frac{1}{2}$. Then we have*

$$|\mathcal{E}_n(f)| = |\mathcal{I}(f) - Q_n(f)| \leq C(2\rho)^{-2n} \max_{z \in \partial \Xi^{\rho}} |f^*(z)|. \tag{4.24}$$

4.3 Tensor-Gaussian quadrature

We will now describe the multi-dimensional case. Let the reference domain be the unit cube $\widehat{J} = [0,1]^d \subset \mathbb{R}^d$ for $d \in \mathbb{N}$. Let $\mathbf{x} = (x_1, \ldots, x_d) \in \mathbb{R}^d$ and $f\colon \widehat{J} \to \mathbb{C}$. We approximate the value of the definite integral

$$\mathcal{I}(f) \coloneqq \int_{[0,1]^d} f(\mathbf{x})\, d\mathbf{x} \tag{4.25}$$

by the tensor-Gaussian quadrature of order $\mathbf{n} = (n_1, \ldots, n_d) \in \mathbb{N}^d$, which is defined by

$$Q^d_{\mathbf{n}}(f) \coloneqq Q_{n_1} \otimes \cdots \otimes Q_{n_d}(f) = \sum_{i_1=1}^{n_1} \cdots \sum_{i_d=1}^{n_d} \omega_{i_1} \cdots \omega_{i_d} f(\xi_{i_1}, \ldots, \xi_{i_d}), \tag{4.26}$$

where ω_{i_j} and ξ_{i_j} for $1 \leq j \leq n_j$ are the Gaussian weights and nodes for the one-dimensional domain $[0,1]$.

As before, let us denote the error of the quadrature by

$$\mathcal{E}_{\mathbf{n}}(f) \coloneqq \mathcal{I}(f) - Q^d_{\mathbf{n}}(f). \tag{4.27}$$

We now extend Theorem 5 to the multi-dimensional case [SS11, Theorem 5.3.15].

Definition 7. For $1 \le i \le d$ and $-\infty < a_i < b_i < \infty$, let $\Theta := \bigotimes_{i=1}^{d} [a_i, b_i] \subset \mathbb{R}^d$. A continuous function $f\colon \Theta \to \mathbb{C}$ is called *componentwise analytic* if there exist $(\rho_i)_{i=1}^{d}$ with $\rho_i > \frac{b_i - a_i}{2}$ for $1 \le i \le d$ such that for all $1 \le i \le d$ and all $\mathbf{x} \in \Theta$ the function

$$\begin{aligned} f_{i,\mathbf{x}}\colon [a_i, b_i] &\to \mathbb{C} \\ t &\mapsto f_{i,\mathbf{x}} := f(x_1, \dots, x_{i-1}, t, x_{i+1}, \dots, x_d) \end{aligned} \tag{4.28}$$

has an analytic continuation $f^*_{i,\mathbf{x}}\colon \Xi^{\rho_i}_{a_i,b_i} \to \mathbb{C}$.

Theorem 6. *Let $f\colon [0,1]^d \to \mathbb{C}$ be a componentwise analytic function and $(\rho_i)_{i=1}^{d}$ as in Definition 7. Then, we have the error estimate*

$$|\mathcal{E}_{\mathbf{n}}(f)| \le \sum_{i=1}^{d} C_i (2\rho_i)^{-2n_i} \max_{\mathbf{x} \in [0,1]^d} \max_{z \in \partial \Xi^{\rho_i}} \left| f^*_{i,\mathbf{x}}(z) \right|, \tag{4.29}$$

for the Gaussian quadrature of order $\mathbf{n} = (n_1, \dots, n_d) \in \mathbb{N}^d$.

We will, however, mostly consider quadrature with the same order $n \in \mathbb{N}$ in every direction, i.e. with $\mathbf{n} = (n, \dots, n)$, and write $Q^d_n = Q^d_{\mathbf{n}}$. Moreover, the integration domain is the four-dimensional unit cube, so $d = 4$. In this case, the error estimation can be rewritten as

$$|\mathcal{E}_n(f)| \le \sum_{i=1}^{4} C_i (2\rho_i)^{-2n} \max_{\mathbf{x} \in [0,1]^4} \max_{z \in \partial \Xi^{\rho_i}} \left| f^*_{i,\mathbf{x}}(z) \right| \le \tilde{C} \rho^{-n}, \tag{4.30}$$

where

$$\begin{aligned} \tilde{C} &= 4 \max \left\{ C_i \max_{\mathbf{x} \in [0,1]^4} \max_{z \in \partial \Xi^{\rho_i}} \left| f^*_{i,\mathbf{x}}(z) \right| \right\}, \\ \rho &= \left(2 \max\{\rho_i\}\right)^2. \end{aligned}$$

5 Numerical approximation of the boundary integral

In this section, we present the concrete circumstances under which the experiments were developed.

As seen in Section 3, in order to solve the coupled system (2.8) we have to compute for different z the entries of the Helmholtz matrices in (3.10). They are of the form

$$\big(\mathbf{K}_j(z)\big)_{k,\ell} = \int_\Gamma \int_\Gamma \mathcal{K}(\mathbf{x}-\mathbf{y},z) b_\ell^j(\mathbf{y}) b_k^j(\mathbf{x})\, d\Gamma_y d\Gamma_x, \tag{5.1}$$

where b_k^j, b_ℓ^j are the piecewise constant basis functions defined in (3.8) for the mesh $\mathcal{G}_j$ approximating Γ at time step t_j. $\mathcal{K}(z)\colon \mathbb{R}^3\backslash\{0\} \to \mathbb{C}$ denotes the Laplace transform of the fundamental solution of the wave equation, i.e.

$$\mathcal{K}(\mathbf{x}-\mathbf{y},z) = \frac{\mathrm{e}^{-z\|\mathbf{x}-\mathbf{y}\|}}{4\pi\,\|\mathbf{x}-\mathbf{y}\|}. \tag{5.2}$$

It holds

$$\begin{aligned}\big(\mathbf{K}_j(z)\big)_{k,\ell} &= \sum_{\tau\in\mathcal{G}} \sum_{\tau_*\in\mathcal{G}} \int_\tau \int_{\tau_*} \mathcal{K}(\mathbf{x}-\mathbf{y},z) b_\ell^j(\mathbf{y}) b_k^j(\mathbf{x})\, d\Gamma_y d\Gamma_x \\ &= \int_{\tau_k} \int_{\tau_\ell} \mathcal{K}(\mathbf{x}-\mathbf{y},z)\, d\Gamma_y d\Gamma_x,\end{aligned} \tag{5.3}$$

since, by construction of the basis functions, the integrand is zero whenever $\mathbf{x} \notin \tau_i$ or $\mathbf{y} \notin \tau_j$. Therefore, it is enough to study the quadrature over pairs of triangles.

5.1 Regularizing transforms

In order to compute the integrals efficiently and exactly enough, we have to develop a procedure to avoid the singularities of $\mathcal{K}(\mathbf{x}-\mathbf{y},z)$ when $\tau_k \cap \tau_\ell \neq \emptyset$. This is done in Chapter 5 of [SS11]. We summarize here the main ideas of these regularizing coordinate transforms.

First, the integration over $\tau_k \times \tau_\ell$ is transformed onto the reference element $\hat{\tau}\times\hat{\tau}$ using χ_{τ_k} respectively χ_{τ_ℓ} (cf. (3.5)). The quadrature rule is then applied to this reference element.

Furthermore, relative coordinates $\mathbf{z} = \mathbf{x}-\mathbf{y}$ are introduced with the goal of fixing the singularity of $\|\mathbf{x}-\mathbf{y}\|$ at the origin. Four cases are distinguished:

- identical triangles,
- triangles with a common edge,

- triangles with a common vertex,
- triangles with a positive distance.

For each case, an ϵ-neighbourhood is cut out and a decomposition of the integration domain is chosen. Then, the integration order is changed and the integration domain is transformed onto the four-dimensional unit cube $[0,1]^4$. It is shown that for each case, the integrand can be analytically extended to a complex neighbourhood of $[0,1]^4$. Finally, some assumptions on the parametrization of the two triangles have to be made.

Assumption 7. Let be $\tau, \tau_* \in \mathcal{G}$ and χ_τ, χ_{τ_*} be their parametrizations.

- In the case of identical panels, it holds $\chi_\tau = \chi_{\tau_*}$.
- In the case of a common edge, it holds $\chi_\tau(\xi,0) = \chi_{\tau_*}(\xi,0)\ \forall \xi \in [0,1]$.
- In the case of a common vertex, it holds $\chi_\tau(0,0) = \chi_{\tau_*}(0,0)$.

For $\hat{\mathbf{x}}, \hat{\mathbf{y}} \in [0,1]^2$, we can now define the integrand in local coordinates [see SS11, Chapter 5.2.4]

$$\mathcal{K}_z^{\mathrm{loc}}(\hat{\mathbf{x}}, \hat{\mathbf{y}}) = \mathcal{K}(\chi_\tau(\hat{\mathbf{x}}) - \chi_{\tau_*}(\hat{\mathbf{y}}), z) g_\tau(\hat{\mathbf{x}}) g_{\tau_*}(\hat{\mathbf{y}}), \tag{5.4}$$

where g_τ denotes the Gram determinant of χ_τ,

$$g_\tau(\hat{x}) = \sqrt{\det(D\chi_\tau(\hat{\mathbf{x}}))^T (D\chi_\tau(\hat{\mathbf{x}}))}. \tag{5.5}$$

Note that $D\chi_\tau(\hat{\mathbf{x}}) = \mathbf{M}_\tau$ and hence the Gram determinant does not depend on $\hat{\mathbf{x}}$, i.e. is constant:

$$\begin{aligned} g_\tau^2 &= \det(\mathbf{M}_\tau^T \mathbf{M}_\tau) \\ &= \det\left(\begin{pmatrix} \mathbf{B}-\mathbf{A} \\ \mathbf{C}-\mathbf{B} \end{pmatrix} \cdot \left(\mathbf{B}-\mathbf{A} \middle| \mathbf{C}-\mathbf{B}\right)\right) \\ &= \det\begin{pmatrix} \|\mathbf{B}-\mathbf{A}\|^2 & \langle \mathbf{B}-\mathbf{A}, \mathbf{C}-\mathbf{B}\rangle \\ \langle \mathbf{B}-\mathbf{A}, \mathbf{C}-\mathbf{B}\rangle & \|\mathbf{C}-\mathbf{B}\|^2 \end{pmatrix} \\ &= \|\mathbf{B}-\mathbf{A}\|^2 \|\mathbf{C}-\mathbf{B}\|^2 - \langle \mathbf{B}-\mathbf{A}, \mathbf{C}-\mathbf{B}\rangle^2 \\ &= 4|\tau|^2. \end{aligned} \tag{5.6}$$

We now introduce the regularizing transforms for the different cases.

Identical triangles

$$\begin{aligned}\mathcal{I}_{\tau\times\tau_*} = \int_{(0,1)^4} \xi^3\eta_1^2\eta_2 \Bigg\{ & \mathcal{K}_z^{\mathrm{loc}}\left(\xi\begin{pmatrix}1\\ 1-\eta_1+\eta_1\eta_2\\ 1-\eta_1\eta_2\eta_3\\ 1-\eta_1\end{pmatrix}\right) + \mathcal{K}_z^{\mathrm{loc}}\left(\xi\begin{pmatrix}1-\eta_1\eta_2\eta_3\\ 1-\eta_1\\ 1\\ 1-\eta_1+\eta_1\eta_2\end{pmatrix}\right)\\ & + \mathcal{K}_z^{\mathrm{loc}}\left(\xi\begin{pmatrix}1\\ \eta_1(1-\eta_2+\eta_2\eta_3)\\ 1-\eta_1\eta_2\\ \eta_1(1-\eta_2)\end{pmatrix}\right) + \mathcal{K}_z^{\mathrm{loc}}\left(\xi\begin{pmatrix}1-\eta_1\eta_2\\ \eta_1(1-\eta_2)\\ 1\\ \eta_1(1-\eta_2+\eta_2\eta_3)\end{pmatrix}\right)\\ & + \mathcal{K}_z^{\mathrm{loc}}\left(\xi\begin{pmatrix}1-\eta_1\eta_2\eta_3\\ \eta_1(1-\eta_2\eta_3)\\ 1\\ \eta_1(1-\eta_2)\end{pmatrix}\right) + \mathcal{K}_z^{\mathrm{loc}}\left(\xi\begin{pmatrix}1\\ \eta_1(1-\eta_2)\\ 1-\eta_1\eta_2\eta_3\\ \eta_1(1-\eta_2\eta_3)\end{pmatrix}\right)\Bigg\} d\eta_1 d\eta_2 d\eta_3 d\xi.\end{aligned} \tag{5.7}$$

Triangles with a common edge

$$\begin{aligned}\mathcal{I}_{\tau\times\tau_*} = \int_{(0,1)^4} & \xi^3\eta_1^2\mathcal{K}_z^{\mathrm{loc}}\left(\xi\begin{pmatrix}1\\ \eta_1\eta_3\\ 1-\eta_1\eta_2\\ \eta_1(1-\eta_2)\end{pmatrix}\right)\\ & + \xi^3\eta_1^2\eta_2\Bigg\{ \mathcal{K}_z^{\mathrm{loc}}\left(\xi\begin{pmatrix}1\\ \eta_1\\ 1-\eta_1\eta_2\eta_3\\ \eta_1\eta_2(1-\eta_3)\end{pmatrix}\right) + \mathcal{K}_z^{\mathrm{loc}}\left(\xi\begin{pmatrix}1-\eta_1\eta_2\\ \eta_1(1-\eta_2)\\ 1\\ \eta_1\eta_2\eta_3\end{pmatrix}\right)\\ & + \mathcal{K}_z^{\mathrm{loc}}\left(\xi\begin{pmatrix}1-\eta_1\eta_2\eta_3\\ \eta_1\eta_2(1-\eta_3)\\ 1\\ \eta_1\end{pmatrix}\right) + \mathcal{K}_z^{\mathrm{loc}}\left(\xi\begin{pmatrix}1-\eta_1\eta_2\eta_3\\ \eta_1(1-\eta_2\eta_3)\\ 1\\ \eta_1\eta_2\end{pmatrix}\right)\Bigg\} d\eta_1 d\eta_2 d\eta_3 d\xi.\end{aligned} \tag{5.8}$$

Triangles with a common vertex or positive distance

$$\mathcal{I}_{\tau\times\tau_*} = \int_{(0,1)^4} \xi^3\eta_1 \Bigg\{ \mathcal{K}_z^{\mathrm{loc}}\left(\xi\begin{pmatrix}1\\ \eta_1\\ \eta_2\\ \eta_2\eta_3\end{pmatrix}\right) + \mathcal{K}_z^{\mathrm{loc}}\left(\xi\begin{pmatrix}\eta_2\\ \eta_2\eta_3\\ 1\\ \eta_1\end{pmatrix}\right)\Bigg\} d\eta_1 d\eta_2 d\eta_3 d\xi. \tag{5.9}$$

Let us denote the integrands for the different cases by $f(\xi, \eta_1, \eta_2, \eta_3)$. Since $f\colon [0,1]^4 \to \mathbb{C}$ is analytic, we can employ a Tensor-Gaussian quadrature (cf. Section 4.3) to approximate the value of the integral. We will use a four-dimensional Gaussian quadrature with n points in every direction. Let $\omega_1, \ldots, \omega_n$ be the weights and $\xi_1, \ldots, \xi_n$ be the nodes for the interval $[0,1]$. Then,

$$\begin{aligned} \mathcal{I}(f) &= \int_{(0,1)^4} f(\xi, \eta_1, \eta_2, \eta_3) d\eta_1 d\eta_2 d\eta_3 d\xi \\ &\approx \sum_{i=1}^{n} \sum_{j=1}^{n} \sum_{k=1}^{n} \sum_{l=1}^{n} \omega_i \omega_j \omega_k \omega_l f(\xi_i, \xi_j, \xi_k, \xi_l) = Q_n^4(f). \end{aligned} \tag{5.10}$$

In practice, the Gauss weights and nodes are computed once and saved in a file. During the experiments, the program loads the weights and nodes for the desired order and approximates the integral.

5.2 Positioning of the triangles

As said before, we consider four different cases for the positioning of the triangles: identical triangles, triangles with a common edge, triangles with a common vertex and triangles with a positive distance. For the experiments, we will vary the diameter h_τ of the triangles. Specifically, the two triangles $\tau_1 = \operatorname{conv}\{A_1, B_1, C_1\}$ and $\tau_2 = \operatorname{conv}\{A_2, B_2, C_2\}$ are defined as follows:

Identical triangles

$$A_1 = \begin{pmatrix} 0 \\ 0 \\ 0 \end{pmatrix} = A_2, \quad B_1 = \begin{pmatrix} h_\tau \\ 0 \\ 0 \end{pmatrix} = B_2, \quad C_1 = \begin{pmatrix} 0 \\ h_\tau \\ 0 \end{pmatrix} = C_2.$$

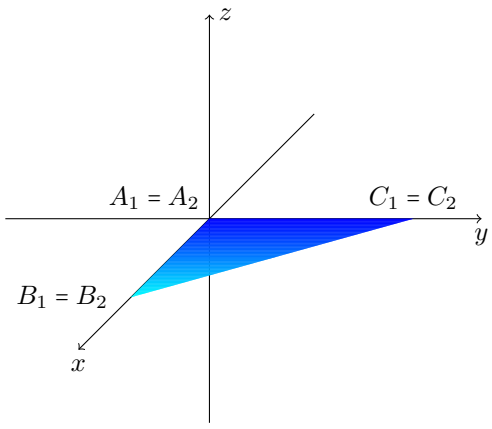

Figure 5.1: Position of the identical triangles.

Triangles with a common edge

$$A_1 = \begin{pmatrix} h_\tau \\ 0 \\ 0 \end{pmatrix} = A_2, \quad B_1 = \begin{pmatrix} 0 \\ h_\tau \\ 0 \end{pmatrix} = B_2, \quad C_1 = \begin{pmatrix} 0 \\ 0 \\ 0 \end{pmatrix}, \quad C_2 = \begin{pmatrix} h_\tau \\ h_\tau \\ 0 \end{pmatrix}.$$

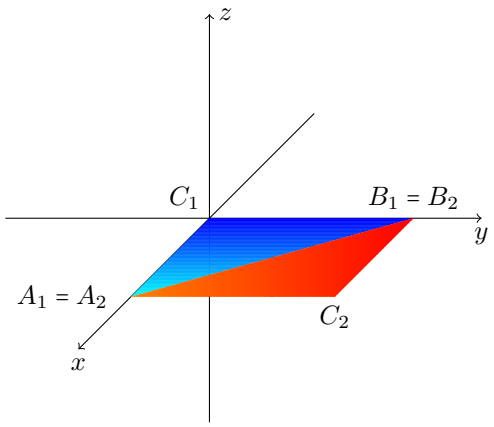

Figure 5.2: Position of the triangles with a common edge.

Triangles with a common vertex

$$A_1 = \begin{pmatrix} 0 \\ 0 \\ 0 \end{pmatrix} = A_2, \quad B_1 = \begin{pmatrix} h_\tau \\ 0 \\ 0 \end{pmatrix}, \quad B_2 = \begin{pmatrix} -h_\tau \\ h_\tau \\ 0 \end{pmatrix}, \quad C_1 = \begin{pmatrix} h_\tau \\ h_\tau \\ 0 \end{pmatrix}, \quad C_2 = \begin{pmatrix} -h_\tau \\ 0 \\ 0 \end{pmatrix}.$$

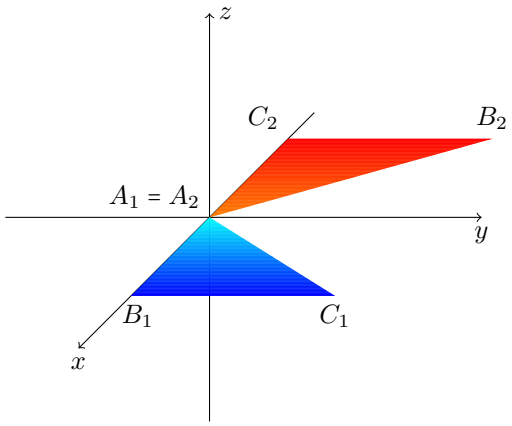

Figure 5.3: Position of the triangles with a common vertex.

Triangles with positive distance

$$A_1 = \begin{pmatrix} 0 \\ 0 \\ 0 \end{pmatrix}, \quad B_1 = \begin{pmatrix} h_\tau \\ 0 \\ 0 \end{pmatrix}, \quad C_1 = \begin{pmatrix} 0 \\ h_\tau \\ 0 \end{pmatrix},$$

$$A_2 = \begin{pmatrix} 0 \\ 0 \\ d \end{pmatrix}, \quad B_2 = \begin{pmatrix} 0 \\ 0 \\ h_\tau + d \end{pmatrix}, \quad C_2 = \begin{pmatrix} h_\tau \\ 0 \\ h_\tau + d \end{pmatrix}.$$

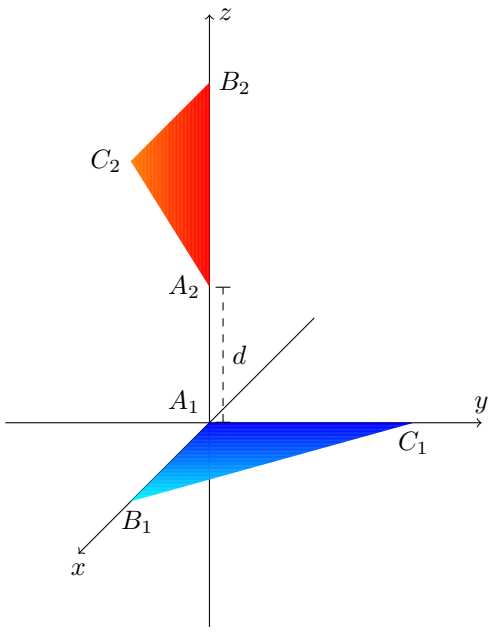

Figure 5.4: Position of the triangles with positive distance d.

In practice, for the numerical experiments, we set $h_\tau \in \{1, 0.1, 0.01\}$ and $d \in \{0.1, 1, 10, 100\}$.

5.3 Complex parameter z

As we have seen in Subsection 3.4, in order to solve the contour integral (3.14), we have to compute the entries of the Helmholtz matrices $(\mathbf{K}_{j+1}(z))_{k,\ell}$ for different z. For both uniform and non-uniform time steps, we choose as a contour a circle centered in M with radius M, where M is defined as in (3.16). This means that the complex parameter z lies on this circle. Note that M

depends on the time discretization. In practice, for the numerical experiments, we take different values of M depending on the diameter of the triangles and analyze the error of the quadrature for five concrete complex numbers on the circle, namely

$$z \in \left\{ M(1 + e^{i\varphi}) \,\middle|\, \varphi = 0, \frac{\pi}{4}, \frac{\pi}{2}, \frac{3\pi}{4}, \pi \right\}, \tag{5.11}$$

for

$$M \in \{h^\ell \mid \ell = -3, -2.5, -2, \ldots, 1, 1.5, 2\}. \tag{5.12}$$

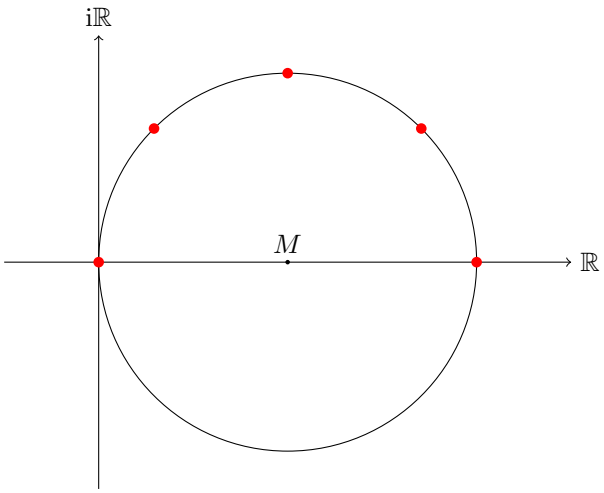

Figure 5.5: Position of the complex parameter z on the contour.

Note that there are no z with negative imaginary parts, because the values of $\mathcal{K}(x, z)$ are symmetric with respect to the real axis.

6 Implementation

In this section, we present the main programs for the numerical experiments and the stored data files. They were implemented in MATLAB.

6.1 Programs

Function: `generate_gauss_XW.m`

Input: ∘ `N` $\in \mathbb{N}$

Output:
- `X`, $n \times 4$ matrix
- `W`, $n \times 1$ vector

Description: This function generates an $n \times 4$ matrix `X` and an $n \times 1$ vector `W`, which are the Gauss nodes respectively the Gauss weights for a 4-dimensional Gaussian quadrature over the unit cube $[0,1]^4$ with `N` points in every direction, i.e. $n = \texttt{N}^4$.
`X` and `W` are then saved to the file '`Gauss_Nodes_Weights.mat`' as `X_N` and `W_N` for the input parameter `N`, so that they have to be computed only once. They can be loaded using the program '`load_gauss_XW.m`'.

Function: `load_gauss_XW.m`

Input: ∘ `N` $\in \mathbb{N}$

Output:
- `X`, $n \times 4$ matrix
- `W`, $n \times 1$ vector

Description: This function loads an $n \times 4$ matrix `X` and an $n \times 1$ vector `W`, which are the Gauss nodes respectively the Gauss weights for a 4-dimensional Gaussian quadrature over $[0,1]^4$ with `N` points in every direction, i.e. $n = \texttt{N}^4$. `X` and `W` are previously generated with the program '`generate_gauss_XW.m`' and saved in '`Gauss_Nodes_Weights.mat`' as `X_N` and `W_N` for the input parameter `N`.

Function: `K_x_z_handle.m`

Input: -

Output:
- `K` as function handle for $\mathcal{K}(r, z)$

Description: This program defines the function handle for the Laplace transform of the fundamental solution of the wave equation defined in (2.5). The function handle then takes following input parameters:

- $z \in \mathbb{C}$
- $r \in \mathbb{R}^3$, or $(r_\ell)_{\ell=1}^n$ (i.e. n different vectors in $\mathbb{R}^3$)

Function: `eval_kernel_fct.m`

Input:
- `x1`, `x2`, `y1`, `y2` such that $\hat{\mathbf{x}} = (\texttt{x1}, \texttt{x2})$ and $\hat{\mathbf{y}} = (\texttt{y1}, \texttt{y2})$ (or four $n \times 1$ vectors for multiple entries)
- `A1`, `B1`, `C1` vertices of the triangle τ, as 3×1 vectors
- `A2`, `B2`, `C2` vertices of the triangle τ_*, as 3×1 vectors
- `z` complex parameter

Output:
- `K_loc` as $\mathcal{K}(\chi_\tau(\hat{\mathbf{x}}) - \chi_{\tau_*}(\hat{\mathbf{y}}), z)$ (cf. (5.4))

Description: This program evaluates the integrand $\mathcal{K}_z^{\text{loc}}$ as seen in equation (5.4) in local coordinates $\mathbf{x} = (\texttt{x1}, \texttt{x2})$, $\mathbf{y} = (\texttt{y1}, \texttt{y2})$. Note that, since $g_\tau(\hat{\mathbf{x}})$ is equal $\forall \hat{\mathbf{x}} \in \tau$, in this program we do not multiply by the Gramian determinants for each pair of local coordinates $\mathbf{x}, \mathbf{y}$. Instead, we later multiply by $g_\tau(\hat{\mathbf{x}}) g_{\tau_*}(\mathbf{y})$ once for all the $\mathbf{x} \in \tau, \mathbf{y} \in \tau_*$.

Function: `eval_identical_panels.m`
`eval_common_edge.m`
`eval_common_vertex.m`

Input:
- `xi`, `eta1`, `eta2`, `eta3` local coordinates (or four $n \times 1$ vectors for multiple entries)
- `A1`, `B1`, `C1` vertices of the triangle τ, as 3×1 vectors
- `A2`, `B2`, `C2` vertices of the triangle τ_*, as 3×1 vectors
- `z` complex parameter

Output:
- `integrand`, scalar (or $n \times 1$ vector)

Description: These programs compute the regularizing transform (5.7), (5.8), respectively (5.9) presented in Subsection 5.1 and then evaluate the integrands for the local coordinates $\xi, \eta_1, \eta_2, \eta_3$.

Function: `quadrature_id_panels.m`
`quadrature_common_edge.m`
`quadrature_common_vertex.m`
`quadrature_positive_distance.m`

Input:
- `h`, diameter of the triangles
- `z`, complex parameter
- `N`, number of Gaussian points in each direction

Output:
- `Q`, approximated value of the integral

Description: These programs approximate the integrals presented in equations (5.7), (5.8), (5.9) for two given triangles in one of the four different configurations (cf. Subsection 5.2). The approximated values are computed using a tensor-Gaussian quadrature with `N` points in each direction.

The algorithms `quadrature_`⟨`case`⟩`.m` for the four different configurations of the triangles have the following structure.

Algorithm 1 `quadrature_⟨case⟩.m`

Generate triangles' vertices $A_1, B_1, C_1, A_2, B_2, C_2$
Compute Gramian determinants g_{τ_1}, g_{τ_2}
$[X_N, W_N]$ = `load_gauss_XW`(N) ▷ load Gaussian weights and nodes
I =`eval_`$\langle$`case`$\rangle(X_N, A_1, B_1, C_1, A_2, B_2, C_2, z)$
$Q = g_{\tau_1} g_{\tau_2} \sum(I \cdot W_N)$;

6.2 Data files

Many different experiments have been conducted. Some of them are presented in Section 7. The approximated values of the integrals computed with the programs `quadrature_`$\langle$`case`$\rangle$`.m` were systematically stored in the files

`id_panels.mat`
`common_edge.mat`
`common_vertex.mat`
`positive_distance.mat`

One can load the data sets using the program `load_quadrature.m`. They are saved for the following parameters:

Parameter	Values
h	$1, 10^{-1}, 10^{-2}$
M	h^l for $l \in \{-3, -2.5, -2, \ldots, 1, 1.5, 2\}$
z	$M(1 + e^{i\varphi}), \varphi = 0, \frac{\pi}{4}, \frac{\pi}{2}, \frac{3\pi}{4}, \pi$
N	$1, \ldots, 80$

Table 6.1: Parameters for the quadrature.

Note that when the diameter h of the triangles is 1, the radius M is always 1. In the configurations with two distinct triangles we have an additional parameter, which is the distance between these two triangles, denoted by d. For this parameter the possible values are $\{10^{-1}, 1, 10\}$.

7 Numerical experiments

With the settings presented in Section 5, we approximate the integral (5.3) by a quadrature. The parameters for this quadrature can be found in Table 6.1. In this section, we report some results about the error. We recall the error estimation presented in Section 4:

$$|\mathcal{E}_n(f)| \leq \tilde{C}\rho^{-n}. \tag{7.1}$$

We first present in detail the results for the case of identical triangles. The behaviour of the error for the other configurations is similar and hence fewer plots and tables are shown.

Since there is no analytical solution, the error is given with regards to a reference solution, which was computed by the Gaussian quadrature with 80 nodes in every direction.

7.1 Identical triangles

7.1.1 Triangle diameter $h = 1$

Figure 7.1 shows the relative error and the estimated linear fitting for $z = 1 + e^{i\frac{\pi}{4}}$. The machine error is reached with fewer than 20 Gaussian points. The error plots for the other values of z are similar.

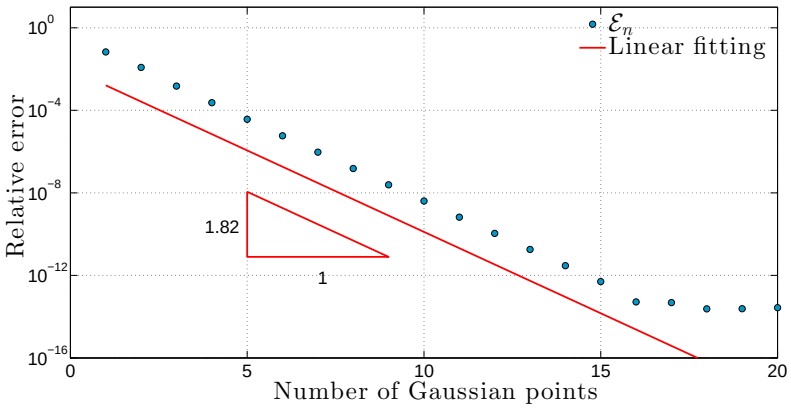

Figure 7.1: Relative error for $h = 1$, $M = 1$ and $z = 1 + e^{i\frac{\pi}{4}}$. $\rho = 6.15$, $\tilde{C} = 0.32$.

The error converges exponentially like the theory suggests (cf. (7.1)). Table 7.1 shows the values of the constants ρ and $\tilde{C}$ of the theoretical error estimate for

the different arguments φ of the considered values z. These are approximated using linear regression on the errors up to machine accuracy, e. g. the first 16 points in Figure 7.1.

φ	ρ	$\tilde{C}$
0	4.91	0.21
$\frac{\pi}{4}$	6.15	0.32
$\frac{\pi}{2}$	6.22	0.32
$\frac{3\pi}{4}$	6.19	0.26
π	6.21	0.24

Table 7.1: Approximated values of ρ and $\tilde{C}$ for $h = 1$.

7.1.2 Triangle diameter $h = 0.1$

With smaller h and $M \leq 10^2$, the error behaves similarly (see Figure 7.2).

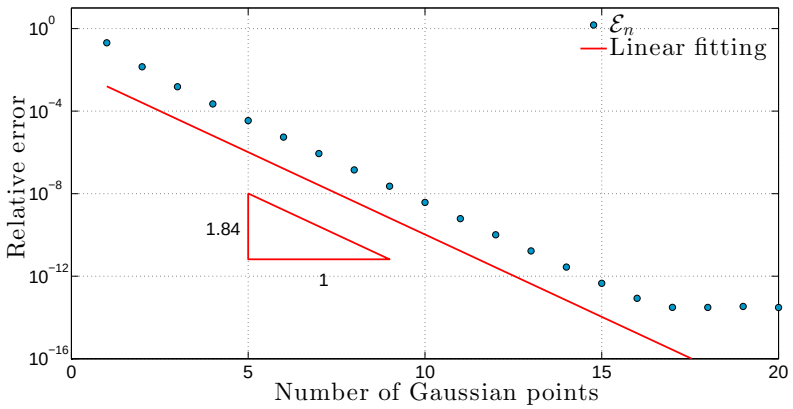

Figure 7.2: Relative error for $h = 0.1$, $M = 10^{1.5}$ and $z = M(1 + e^{i\frac{3\pi}{4}})$. $\rho = 6.28$, $\tilde{C} = 0.38$.

Tables 7.2 and 7.3 show the approximated values of ρ and $\tilde{C}$ respectively for the same values of M. Note that for the special case $\varphi = \pi$, i. e. when $z = 0$, the value of the integral does not depend on M.

	M								
	10^2	$10^{1.5}$	10^1	$10^{0.5}$	10^0	$10^{-0.5}$	10^{-1}	$10^{-1.5}$	10^{-2}
$\varphi = 0$	5.09	6.08	4.92	6.18	6.22	6.19	6.19	6.18	6.18
$\varphi = \frac{\pi}{4}$	5.96	6.10	6.15	6.21	6.19	6.17	6.20	6.21	6.20
$\varphi = \frac{\pi}{2}$	5.96	6.19	6.21	6.18	6.17	6.19	6.20	6.17	6.21
$\varphi = \frac{3\pi}{4}$	6.13	6.28	6.17	6.19	6.22	6.18	6.20	6.20	6.20
$\varphi = \pi$					6.19				

Table 7.2: Approximated values of ρ for $h = 0.1$.

	M								
	10^2	$10^{1.5}$	10^1	$10^{0.5}$	10^0	$10^{-0.5}$	10^{-1}	$10^{-1.5}$	10^{-2}
$\varphi = 0$	0.44	0.52	0.21	0.27	0.26	0.24	0.24	0.23	0.24
$\varphi = \frac{\pi}{4}$	0.71	0.50	0.32	0.28	0.25	0.23	0.24	0.24	0.24
$\varphi = \frac{\pi}{2}$	0.68	0.49	0.32	0.25	0.24	0.24	0.24	0.23	0.24
$\varphi = \frac{3\pi}{4}$	0.64	0.38	0.25	0.24	0.25	0.24	0.24	0.24	0.24
$\varphi = \pi$					0.24				

Table 7.3: Approximated values of $\tilde{C}$ for $h = 0.1$.

For $M > 10^2$, the convergence rate seems to become superexponential (see for example the error plot for $M = 10^3$ in Figure 7.3), i.e.

$$\mathcal{E}_n \leq \tilde{C}\rho^{-N^\alpha} \tag{7.2}$$

for some $\alpha > 1$. However, the parameter ρ approaches 1 and hence more Gaussian points are needed to reach the machine error. Notice that the exponential convergence corresponds to the case $\alpha = 1$.

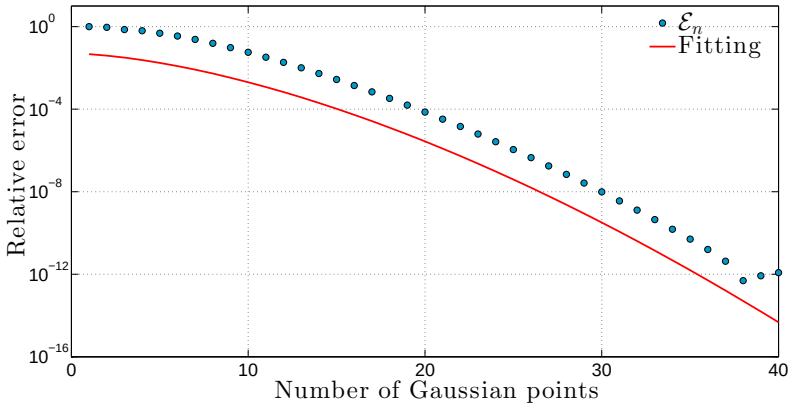

Figure 7.3: Relative error for $h = 0.1$, $M = 10^3$ and $z = M(1 + e^{i\frac{\pi}{4}})$. $\rho = 1.09$, $\tilde{C} = 1.4$, $\alpha = 1.59$.

Table 7.4 shows the approximated values of the constants $\rho, \tilde{C}$ and α for $M = 10^3$ or $10^{2.5}$.

	ρ		$\tilde{C}$		α	
M	10^3	$10^{2.5}$	10^3	$10^{2.5}$	10^3	$10^{2.5}$
$\varphi = 0$	1.09	1.29	1.41	1.58	1.59	1.52
$\varphi = \frac{\pi}{4}$	1.09	1.29	1.40	1.55	1.59	1.53
$\varphi = \frac{\pi}{2}$	1.10	1.34	1.43	1.86	1.58	1.51
$\varphi = \frac{3\pi}{4}$	1.13	1.47	2.51	3.80	1.56	1.54

Table 7.4: Approximated values of ρ, $\tilde{C}$ and α for $h = 0.1$.

7.1.3 Triangle diameter $h = 0.01$

The results for $h = 0.01$ are very similar: For $M \leq 10^3$ the convergence is exponential; for bigger M it is superexponential. In this case however, ρ tends to 1 and therefore the effect of the exponent $\alpha > 1$ is neutralized.

Tables 7.5, 7.6 and 7.7 show the approximated values of the constants $\rho, \tilde{C}$ and α for the different M and φ.

	M							
	10^3	10^2	10^1	10^0	10^{-1}	10^{-2}	10^{-3}	10^{-4}
$\varphi = 0$	4.60	4.93	6.19	6.18	6.20	6.18	6.20	6.19
$\varphi = \frac{\pi}{4}$	5.84	6.15	6.20	6.17	6.19	6.20	6.19	6.20
$\varphi = \frac{\pi}{2}$	5.92	6.21	6.17	6.20	6.19	6.19	6.18	6.19
$\varphi = \frac{3\pi}{4}$	6.15	6.18	6.22	6.20	6.18	6.19	6.18	6.20
$\varphi = \pi$	6.21							

Table 7.5: Approximated values of ρ for $h = 0.01$.

	M							
	10^3	10^2	10^1	10^0	10^{-1}	10^{-2}	10^{-3}	10^{-4}
$\varphi = 0$	0.44	0.21	0.25	0.24	0.24	0.23	0.24	0.24
$\varphi = \frac{\pi}{4}$	0.56	0.32	0.25	0.23	0.24	0.24	0.24	0.24
$\varphi = \frac{\pi}{2}$	0.63	0.31	0.24	0.24	0.24	0.24	0.24	0.24
$\varphi = \frac{3\pi}{4}$	0.65	0.25	0.25	0.24	0.23	0.24	0.23	0.24
$\varphi = \pi$	0.24							

Table 7.6: Approximated values of $\tilde{C}$ for $h = 0.01$.

	ρ			α		
M	10^6	10^5	10^4	10^6	10^5	10^4
$\varphi = 0$	1.0004	1.0019	1.086	2.03	2.10	1.59
$\varphi = \frac{\pi}{4}$	1.0004	1.0017	1.082	2.03	2.13	1.61
$\varphi = \frac{\pi}{2}$	1.0002	1.0012	1.102	2.15	2.22	1.57
$\varphi = \frac{3\pi}{4}$	1.0002	1.0102	1.168	2.13	1.74	1.49

Table 7.7: Approximated values of ρ and α for $h = 0.01$.

7.1.4 Variation of the integral value

We now observe how the value of the computed integral varies for the different z. Our aim is to study, how the value of the integral is influenced by the radius M and by the complex parameter z.

Let us denote by $Q(h, z)$ the approximated value of the integral. For a fixed h, the maximum value is always attained at $z = 0$ (i.e. $\varphi = \pi$).

Table 7.8 shows the ratio between $|Q(h, z)|$ and $|Q(h, 0)|$. Notice that the bigger M is, the smaller the ratio becomes.

	φ	0	$\frac{\pi}{4}$	$\frac{\pi}{2}$	$\frac{3\pi}{4}$	π
h = 1						
		0.6523	0.6842	0.7816	0.9223	1
h = 0.1						
	$M = 10^{-2}$	0.9995	0.9996	0.9998	0.9999	1
	$10^{-1.5}$	0.9984	0.9987	0.9992	0.9998	1
	10^{-1}	0.9950	0.9958	0.9975	0.9993	1
	$10^{-0.5}$	0.9844	0.9867	0.9922	0.9977	1
	10^{0}	0.9522	0.9588	0.9754	0.9926	1
	$10^{0.5}$	0.8609	0.8784	0.9243	0.9764	1
	10^{1}	0.6523	0.6842	0.7816	0.9223	1
	$10^{1.5}$	0.3552	0.3826	0.4865	0.7438	1
	10^{2}	0.1405	0.1521	0.1986	0.3656	1
	$10^{2.5}$	0.0479	0.0518	0.0677	0.125	1
	10^{3}	0.0155	0.0168	0.0219	0.0405	1
h = 0.01						
	$M = 10^{-4}$	1.0000	1.0000	1.0000	1.0000	1
	10^{-3}	1.0000	1.0000	1.0000	1.0000	1
	10^{-2}	0.9999	0.9999	0.9999	0.9999	1
	10^{-1}	0.9995	0.9996	0.9998	0.9999	1
	10^{0}	0.9950	0.9958	0.9975	0.9993	1
	10^{1}	0.9521	0.9588	0.9754	0.9926	1
	10^{2}	0.6523	0.6842	0.7816	0.9223	1
	10^{3}	0.1405	0.1521	0.1986	0.3656	1
	10^{4}	0.0155	0.0168	0.0219	0.0405	1
	10^{5}	0.0016	0.0017	0.0022	0.0041	1
	10^{6}	9.3e-05	0.0001	0.0002	0.0005	1

Table 7.8: Ratio $\frac{|Q(h,z)|}{|Q(h,0)|}$ for different values of h, M and z.

7.2 Triangles with a common edge

The error behaves as in the previous case. Therefore, only some tables with the approximated values of the constants $\tilde{C}$, ρ and α are reported.

7.2.1 Triangle diameter $h = 1$

φ	ρ	$\tilde{C}$
0	6.92	0.14
$\frac{\pi}{4}$	7.02	0.14
$\frac{\pi}{2}$	7.12	0.12
$\frac{3\pi}{4}$	7.27	0.11
π	7.25	0.09

Table 7.9: Approximated values of ρ and $\tilde{C}$ for $h = 1$.

7.2.2 Triangle diameter $h = 0.1$

The superexponential convergence rate arises for $M \geq 10^2$.

	ρ			α		
M	10^3	$10^{2.5}$	10^2	10^3	$10^{2.5}$	10^2
$\varphi = 0$	1.0147	1.0947	1.1135	2.03	1.81	2.08
$\varphi = \frac{\pi}{4}$	1.0118	1.1503	1.2867	2.09	1.69	1.75
$\varphi = \frac{\pi}{2}$	1.0000	1.0227	2.1769	3.68	2.30	1.35
$\varphi = \frac{3\pi}{4}$	1.0069	1.1068	6.9001	2.31	1.98	1.00

Table 7.10: Approximated values of ρ and α for $h = 0.1$.

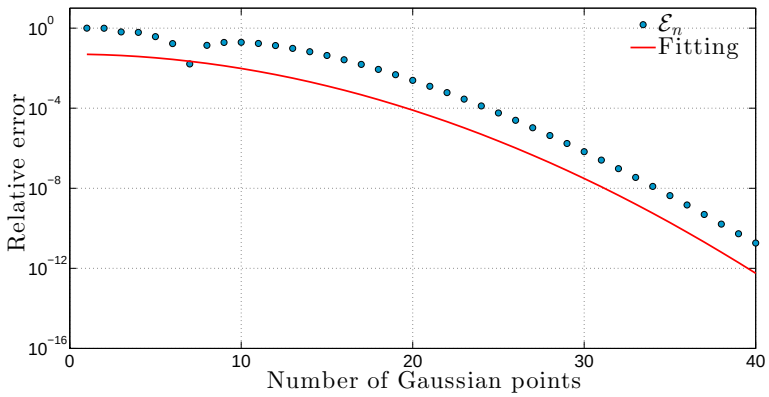

Figure 7.4: Relative error for $h = 0.1$, $M = 10^3$ and $z = 2M$.
$\rho = 1.0147$, $\tilde{C} = 1.36$, $\alpha = 2.03$.

7.2.3 Triangle diameter $h = 0.01$

With diameter $h = 0.01$, the superexponential convergence rate arises for $M \geq 10^3$.

	ρ				α			
M	10^6	10^5	10^4	10^3	10^6	10^5	10^4	10^3
$\varphi = 0$	1.0002	1.0003	1.0146	1.0422	2.21	3.70	2.03	2.47
$\varphi = \frac{\pi}{4}$	1.0001	1.0005	1.0118	1.2028	2.28	3.54	2.09	1.89
$\varphi = \frac{\pi}{2}$	1.0001	1.0092	1.0001	1.9539	2.15	2.42	3.68	1.41
$\varphi = \frac{3\pi}{4}$	1.0000	3.4722	1.0056	6.8799	3.70	1.00	2.38	1.00

Table 7.11: Approximated values of ρ and α for $h = 0.01$.

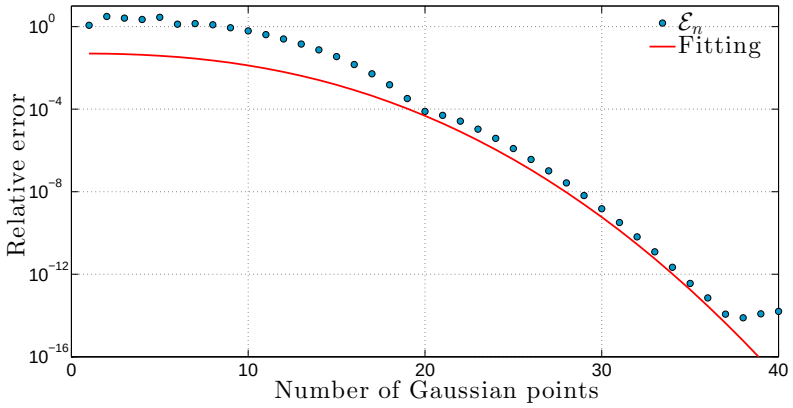

Figure 7.5: Relative error for $h = 0.01$, $M = 10^4$ and $z = M(1 + e^{i\frac{3\pi}{4}})$. $\rho = 1.0056$, $\tilde{C} = 0.13$, $\alpha = 2.38$.

7.2.4 Variation of the integral value

We observe the variation of the integral value along the complex circle. The largest value is again taken in $z = 0$ (i.e. $\varphi = \pi$). Table 7.12 shows the ratio between $|Q(h, z)|$ and $|Q(h, 0)|$.

	φ	0	$\frac{\pi}{4}$	$\frac{\pi}{2}$	$\frac{3\pi}{4}$	π
h = 1						
		0.3973	0.4431	0.5969	0.8494	1
h = 0.1						
$M = 10^{-2}$		0.9990	0.9991	0.9995	0.9998	1
$10^{-1.5}$		0.9967	0.9972	0.9984	0.9995	1
10^{-1}		0.9897	0.9912	0.9948	0.9985	1
$10^{-0.5}$		0.9679	0.9725	0.9838	0.9952	1
10^{0}		0.9028	0.9162	0.9496	0.9849	1
$10^{0.5}$		0.7294	0.7617	0.8492	0.9521	1
10^{1}		0.3973	0.4431	0.5969	0.8494	1
$10^{1.5}$		0.1000	0.1179	0.2058	0.5525	1
10^{2}		0.0131	0.0154	0.0265	0.0954	1
$10^{2.5}$		0.0014	0.0017	0.0028	0.0097	1
10^{3}		0.0001	0.0002	0.0003	0.0010	1
h = 0.01						
$M = 10^{-4}$		1	1	1	1	1
10^{-3}		0.9999	0.9999	0.9999	1	1
10^{-2}		0.9999	0.9999	0.9999	0.9999	1
10^{-1}		0.9989	0.9991	0.9995	0.9998	1
10^{0}		0.9897	0.9912	0.9948	0.9985	1
10^{1}		0.9028	0.9162	0.9496	0.9848	1
10^{2}		0.3973	0.4431	0.5969	0.8494	1
10^{3}		0.0131	0.0154	0.0264	0.0954	1
10^{4}		0.0002	0.0002	0.0003	0.0009	1
10^{5}		1.4e-06	1.7e-06	2.9e-06	9.9e-06	1
10^{6}		1.1e-08	1.4e-08	3.8e-08	2.7e-07	1

Table 7.12: Ratio $\frac{|Q(h,z)|}{|Q(h,0)|}$ for different values of h, M and z.

7.3 Triangles with a common vertex

For triangles with a common vertex, the constant ρ for the exponential convergence is much larger. Moreover, the superexponential convergence arises already for $h = 1$ (cf. Table 7.13).

7.3.1 Triangle diameter $h = 1$

φ	ρ	$\tilde{C}$	α
0	1.5178	0.20	2.02
$\frac{\pi}{4}$	2.1347	0.58	1.73
$\frac{\pi}{2}$	4.0747	1.39	1.47
$\frac{3\pi}{4}$	47.177	5.13	-
π	36.319	0.55	-

Table 7.13: Approximated values of ρ, $\tilde{C}$ and α for $h = 1$.

7.3.2 Triangle diameter $h = 0.1$

In these cases, we notice from the plots that there is a pre-asymptotical behaviour of the error. For this reason, we cannot consider the first few points of the plot when approximating the constants $\rho, \tilde{C}$ and α.

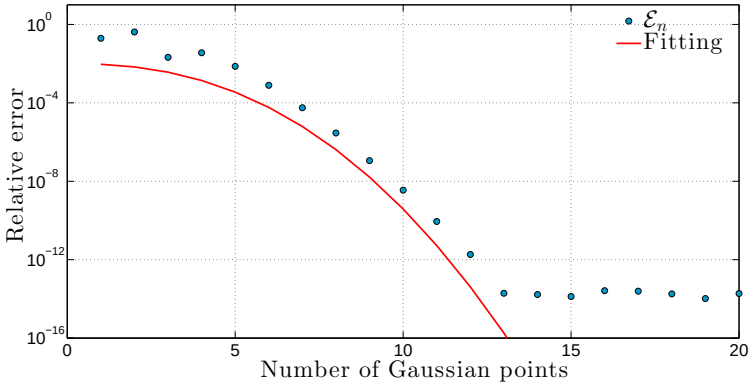

Figure 7.6: Relative error for $h = 0.1$, $M = 10^{1.5}$ and $z = 2M$.
$\rho = 1.0788$, $\tilde{C} = 0.14$, $\alpha = 2.35$.

The approximated values of the constants are reported in Table 7.14. The symbol "-" in the α-fields means that for these cases, the convergence is exponential (i.e. $\alpha = 1$).

		M										
		10^3	$10^{2.5}$	10^2	$10^{1.5}$	10^1	$10^{0.5}$	10^0	$10^{-0.5}$	10^{-1}	$10^{-1.5}$	10^{-2}
ρ												
	$\varphi = 0$	1.0011	1.0084	1.0232	1.0718	1.5096	30.346	31.5383	41.034	39.3131	38.6852	37.6055
	$\frac{\pi}{4}$	1.0003	1.0063	1.0205	1.2401	2.1569	47.6488	40.4372	37.5062	42.8621	37.8635	37.8538
	$\frac{\pi}{2}$	1.0001	1.0007	1.0137	1.5318	3.6599	44.448	40.2568	39.6547	41.2587	36.9109	39.3776
	$\frac{3\pi}{4}$	1.0000	1.0035	1.0681	2.5453	59.0147	42.3912	41.0421	39.027	38.7824	37.8158	40.6902
	π						40.3838					
$\tilde{C}$												
	$\varphi = 0$	1.36	1.56	0.57	0.14	0.17	6.51	0.30	0.98	0.83	0.77	0.69
	$\frac{\pi}{4}$	1.00	1.38	0.33	1.08	0.54	5.65	1.00	0.71	1.13	0.71	0.71
	$\frac{\pi}{2}$	1.00	0.66	0.64	4.05	1.38	2.62	1.04	0.87	0.98	0.64	0.82
	$\frac{3\pi}{4}$	0.40	7.17	7.93	3.25	34.30	1.60	1.03	0.80	0.77	0.70	0.92
	π						0.89					
α												
	$\varphi = 0$	2.49	2.31	2.38	2.40	2.02	1.07	-	-	-	-	-
	$\frac{\pi}{4}$	2.83	2.40	2.43	1.98	1.73	-	-	-	-	-	-
	$\frac{\pi}{2}$	3.31	3.09	2.66	1.78	1.52	-	-	-	-	-	-
	$\frac{3\pi}{4}$	5.60	2.81	2.33	1.59	1.02	-	-	-	-	-	-
	π						-					

Table 7.14: Approximated values of $\rho, \tilde{C}$ and α for $h = 0.1$.

7.3.3 Triangle diameter $h = 0.01$

For $h = 0.01$ and triangles with a common vertex, if $M < 10^4$, we get similar results as before. However, for bigger M, the value of the integral is too small (about 10^{-20}) and this prevents us from computing the error properly.

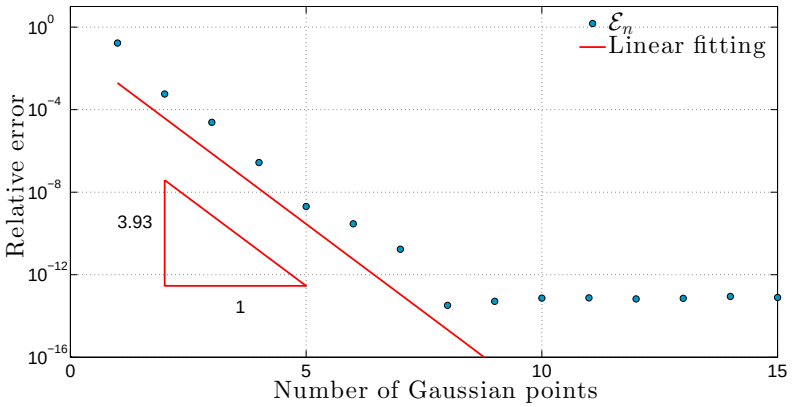

Figure 7.7: Relative error for $h = 0.01$, $M = 10^{-1}$ and $z = M(1 + e^{i\frac{\pi}{4}})$. $\rho = 51.07$, $\tilde{C} = 3.01$.

7.3.4 Variation of the integral value

The variation of the integral value is again very similar as in the case of triangles with a common edge.

7.4 Triangles with positive distance

For distinct triangles, we have the minimal distance $d \in \{0.1, 1, 10\}$ between the triangles as an additional parameter. With this configuration, the case $h = 0.01$ the values of the integrals are very small and thus the quadrature error is strongly influenced by the machine error. For the same reason the radius M has some restriction too.

7.4.1 Triangle diameter $h = 1$

Figures 7.8a, 7.8b and 7.8c show how the distance between the triangles influences the error convergence.

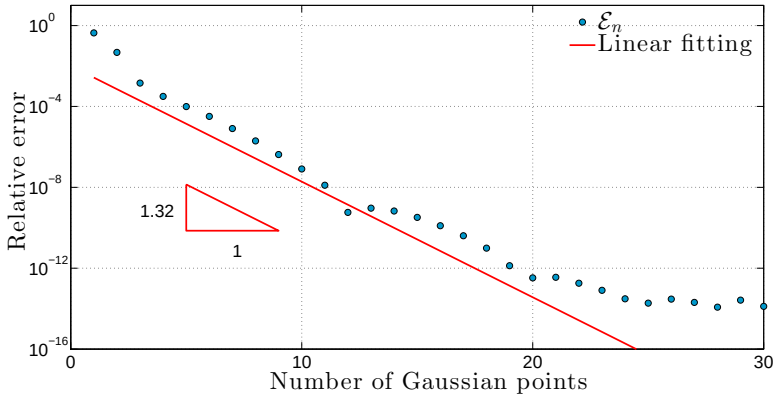

(a) $d = 0.1$.

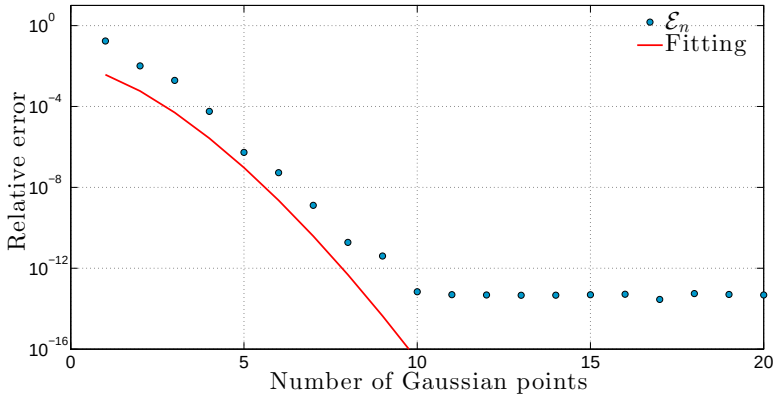

(b) $d = 1$.

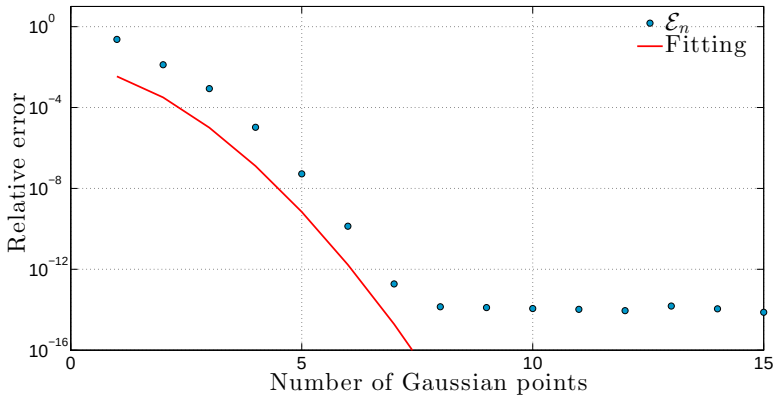

(c) $d = 10$.

Figure 7.8: Relative error for $h = 1$ and $z = 1 + e^{i\frac{\pi}{4}}$.

The approximated values of the constants are reported in Table 7.15. The symbol "-" in the α-fields again means that for these cases, the convergence is exponential ($\alpha = 1$).

d = 0.1		ρ	α
	$\varphi = 0$	3.5254	-
	$\frac{\pi}{4}$	3.5753	-
	$\frac{\pi}{2}$	3.6022	-
	$\frac{3\pi}{4}$	3.5959	-
	π	3.5721	-
d = 1			
	$\varphi = 0$	2.9606	1.42
	$\frac{\pi}{4}$	3.8804	1.36
	$\frac{\pi}{2}$	9.6140	1.17
	$\frac{3\pi}{4}$	28.7161	-
	π	38.8082	-
d = 10			
	$\varphi = 0$	2.1506	1.84
	$\frac{\pi}{4}$	2.8844	1.71
	$\frac{\pi}{2}$	4.1661	1.61
	$\frac{3\pi}{4}$	5.0156	1.65
	π	21.6577	1.48

Table 7.15: Approximated values of ρ and α for $h = 1$.

7.4.2 Triangle diameter $h = 0.1$

Here the results for the case $h = 0.1$ are reported.

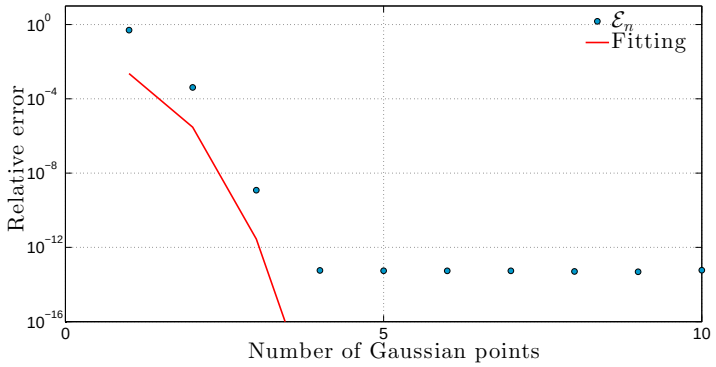

(a) $d = 0.1$.

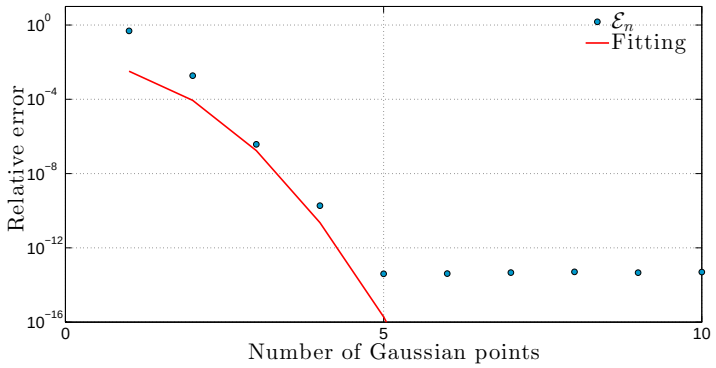

(b) $d = 1$.

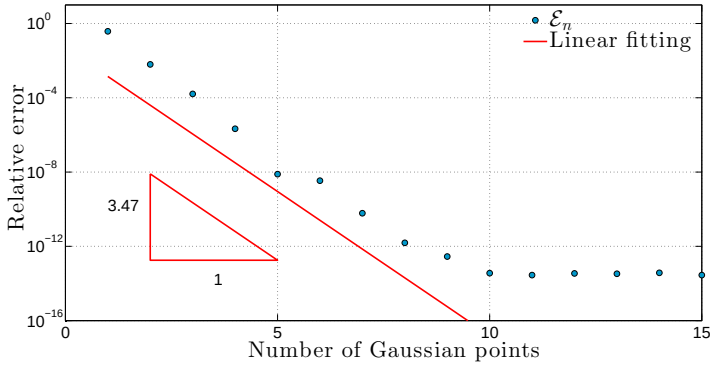

(c) $d = 10$.

Figure 7.9: Relative error for $h = 0.1$, $M = 10^{-1}$ and $z = M(1 + e^{i\frac{\pi}{2}})$.

		M					M				
		10^{0}	$10^{-0.5}$	10^{-1}	$10^{-1.5}$	10^{-2}	10^{0}	$10^{-0.5}$	10^{-1}	$10^{-1.5}$	10^{-2}
d = 0.1				ρ					α		
	$\varphi = 0$	32.4299	31.9334	32.0206	31.931	32.3693	-	-	-	-	-
	$\frac{\pi}{4}$	32.0689	31.8908	32.0465	32.3023	32.3267	-	-	-	-	-
	$\frac{\pi}{2}$	32.0102	32.162	32.0701	32.0656	31.9311	-	-	-	-	-
	$\frac{3\pi}{4}$	32.2077	32.452	32.1716	32.1939	32.6543	-	-	-	-	-
	π			32.1766					-		
d = 1				ρ					α		
	$\varphi = 0$	1.8157	2.3247	9.1351	8.7516	12.5072	2.54	2.24	1.59	1.63	1.51
	$\frac{\pi}{4}$	3.3307	11.2328	9.7634	11.5854	10.5714	1.99	1.61	1.56	1.53	1.57
	$\frac{\pi}{2}$	6.0711	42.9802	9.3929	11.0456	12.5066	1.77	1.32	1.59	1.55	1.51
	$\frac{3\pi}{4}$	12.8994	2.9138	10.1463	10.9673	3.7601	1.59	2.10	1.58	1.56	1.97
	π			10.9157							
d = 10				ρ					α		
	$\varphi = 0$	3.8421	2.6552	9.7459	7.5619	8.7104	2.00	2.42	1.93	2.18	2.17
	$\frac{\pi}{4}$	3.6007	2.5107	9.6437	7.6898	9.0021	2.05	2.47	1.94	2.18	2.16
	$\frac{\pi}{2}$	2.9183	2.2578	11.0071	8.3896	9.9317	2.25	2.59	1.89	2.16	2.12
	$\frac{3\pi}{4}$	2.4347	9.0452	4.6121	9.43	11.3112	2.46	1.96	2.48	2.14	2.08
	π			12.0714					2.05		

Table 7.16: Approximated values of ρ and α for $h = 0.1$.

7.4.3 Variation of the integral value

Again the integral value varies as before for every $d \in \{0.1, 1, 10\}$ and therefore the table is not reported.

8 Conclusion

The experiments we conducted confirm the theory about the error convergence. The conclusions about the experiments are summarized here, together with some ideas for further investigation:

- For general configurations, the error behaves as expected. In some limit cases the convergence is no longer exponential, but even superexponential. However, the base ρ of the exponent $-N^{\alpha}$ tends to 1. This fact neutralize the effect of α. So, in practice, more Gaussian points are needed to achieve the minimal error. One could study in detail the conditions under which this behaviour arises. We can suppose that it depends on the product $h \cdot M$. But how exactly?
- As expected, the configuration of the triangles plays a central role. The approximation works better if there is no singularity in the integrand.
- If the radius M of the complex circle is large, then the value of the integral varies strongly along this circle. Does this mean that, while approximating the quadrature along the complex circle, one could ignore some computations and concentrate on nodes which are near the origin?

References

[Ahl53] L. V. Ahlfors. *Complex Analysis*. International Series in Pure and Applied Mathematics. McGraw-Hill, 1953.

[BHD86] A. Bamberger and T. Ha-Duong. Formulation variationnelle espace-temps pour le calcul par potentiel retardé de la diffraction d'une onde acoustique. *Mathematical Methods in the Applied Sciences*, 8:405–435, 1986.

[EBY99] G. Evans, J. Blackledge, and P. Yardley. *Analytic Methods for Partial Differential Equations*. Graduate Studies in Mathematics. American Mathematical Society, 1999.

[Eva98] G. Evans. *Parital Differential Equations*. Springer Undergraduate Mathematics Series. Springer, 1998.

[Hac92] W. Hackbusch. *Elliptic Differential Equations*. Springer Series in Computational Mathematics. Springer, 1992.

[Jan71] Lothar Jantscher. *Distributionen*. de Gruyter Lehrbuch, 1971.

[LFS12a] M. Lopez-Fernandez and S. Sauter. A Generalized Convolution Quadrature with Variable Time Stepping. 2012.

[LFS12b] M. Lopez-Fernandez and S. Sauter. A Generalized Convolution Quadrature with Variable Time Stepping. Part II: Algorithms and Numerical Results. Technical report, Institut für Mathematik, Universität Zürich, 2012.

[Lub94] C. Lubich. On the Multistep Time Discretization of Linear Initial-Boundary Value Problems and their Boundary Integral Equations. *Numerische Mathematik*, 67:365–389, 1994.

[Sau10] S. Sauter. Lecture notes: Introduction to numerics. 2010.

[Sch12] R. Schnyder. Time and space adaptive solution to retarded potential integral equations. Master's thesis, 2012.

[SS11] S. Sauter and C. Schwab. *Boundary Element Methods*. Springer Series in Computational Mathematics. Springer, 2011.

[Sto07] J. Stoer. *Numerische Mathematik*. Springer-Verlag, Heidelberg, 2007.

A Additional mathematical background

In this appendix, we gather some theoretical frameworks which are helpful for the understanding of the thesis.

A.1 Complex contour integrals

As seen in Subsection 2.3, we have to deal with complex contour integrals. In this subsection, we introduce some basic theory about them, based on [Ahl53].

Definition 8. A *curve* in the complex plane is a continuous map

$$\gamma\colon [a,b] \to \mathbb{C},$$

where $a, b \in \mathbb{R}, a < b$. γ is called *smooth* if it is continuously differentiable, and it is called *closed* if $\gamma(a) = \gamma(b)$.

We define the integral of a continuous complex function along a curve.

Definition 9. Let $\gamma\colon [a,b] \to \mathbb{C}$ be a smooth curve and let $f\colon D \to \mathbb{C}$ be a continuous map, where $D \subset \mathbb{C}$ and $\gamma([a,b]) \subset D$. We define the *contour integral* of f along γ as

$$\int_\gamma f(z)\,dz := \int_a^b f(\gamma(t))\gamma'(t)\,dt.$$

Note that the value of the integral does not depend on the parametrization of the curve, but only on its image and direction.

We now present Cauchy's integral formula, which is a crucial formula in the context of contour integrals. First, we need a definition.

Definition 10. Let γ be a curve and let $z_0 \in \mathbb{C}$. The *winding number* of γ with respect to z_0 is defined by

$$n(\gamma, z_0) = \frac{1}{2\pi \mathrm{i}} \int_\gamma \frac{1}{z - z_0}\,dz. \tag{A.1}$$

$n(\gamma, z_0)$ is sometimes called the *index* of z_0 with respect to γ.

For a curve to have winding number $n > 0$ with respect to a point roughly means that it twists n times around this point; counterclockwise if n is positive, clockwise if n is negative.

Theorem 8 (Cauchy's integral formula)**.** *Let $U \subset \mathbb{C}$ an open subset, $f\colon U \to \mathbb{C}$ a holomorphic function and $\gamma\colon [a,b] \to \mathbb{C}$ a smooth closed curve with image contained in U. Then, for any point z_0 not on γ,*

$$n(\gamma, z_0) \cdot f(z_0) = \frac{1}{2\pi \mathrm{i}} \int_\gamma \frac{f(z)}{z - z_0}\,dz.$$

The easiest application is when $n(\gamma, z_0) = 1$. We then have

$$f(z_0) = \frac{1}{2\pi \mathrm{i}} \int_\gamma \frac{f(z)}{z - z_0}\, dz,$$

which allows us to compute $f(z_0)$ as soon as the values of an analytic function f on γ are known.

Cauchy's integral formula is then generalized to the residue theorem:

Theorem 9 (Residue Theorem)**.** *Let $U \subset \mathbb{C}$ an open subset, $f\colon U \to \mathbb{C}$ a meromorphic function and $\gamma\colon [a,b] \to \mathbb{C}$ a smooth closed curve with image contained in U. Assume the poles of f are given by $\alpha_1, \alpha_2, \ldots, \alpha_\ell$. Then,*

$$\frac{1}{2\pi \mathrm{i}} \int_\gamma f(z)\, dz = \sum_{k=1}^{\ell} n(\gamma, \alpha_k) \operatorname{Res}(f, \alpha_k),$$

where the residue of f at α_k, $k = 1, \ldots, \ell$, is given by

$$\operatorname{Res}(f, \alpha_k) := \frac{1}{2\pi \mathrm{i}} \int_C f(z)\, dz,$$

with $C(t) = \alpha_k + \varepsilon e^{t\mathrm{i}}$ for $0 \le t \le 2\pi$ and ε sufficiently small.[5]

Note that the value of the integral along γ only depends on the winding numbers of the curve around the poles of f.

Let us now look at the special case of the half-plane $U = \{s \in \mathbb{C} \mid \operatorname{Re}(s) > 0\}$ and the map

$$\begin{aligned} \gamma\colon \mathbb{R} &\to \mathbb{C} \\ t &\mapsto \sigma_0 + \mathrm{i}t \end{aligned}$$

with $\sigma_0 > 0$. The definition of the contour integral can be extended to unbounded lines like γ by using an improper integral, and with certain requirements on f, Cauchy's integral formula can also be extended.

Lemma 10. *If $\sup_{z \in U} |z f(z)| < \infty$ and $z_0 \in U$ with $\operatorname{Re}(z_0) > \sigma_0$, then*

$$f(z_0) = -\frac{1}{2\pi \mathrm{i}} \int_\gamma \frac{f(z)}{z - z_0}\, dz.$$

Proof. We employ Cauchy's integral formula for a curve γ_* as in figure A.1. We obtain

$$n(\gamma_*, z_0) \cdot f(z_0) = \frac{1}{2\pi \mathrm{i}} \int_{\gamma_*} \frac{f(z)}{z - z_0}\, dz.$$

[5] The other poles α_j, $j \neq k$, have to be outside the curve C.

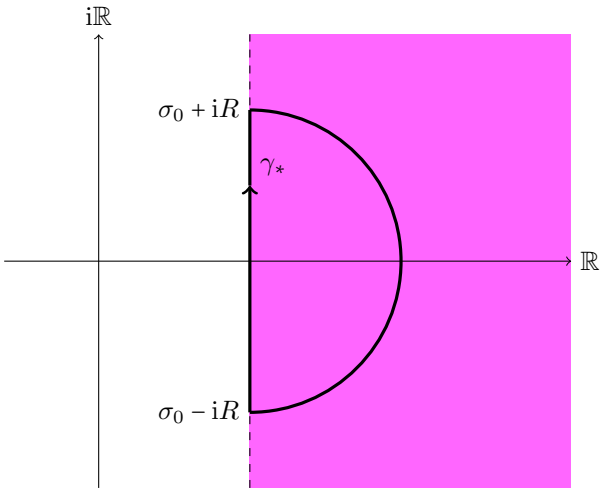

Figure A.1: Extension of Cauchy's integral formula.

For a sufficient large R, we have $n(\gamma_*, z_0) = -1$. Moreover, we can split the integral along the curve as follows:

$$-f(z_0) = \frac{1}{2\pi\mathrm{i}} \left(\int_{-R}^{R} \frac{f(\sigma_0 + \mathrm{i}t)}{\sigma_0 + \mathrm{i}t - z_0} \mathrm{i}\, dt + \int_{\frac{\pi}{2}}^{-\frac{\pi}{2}} \frac{f(R(\sigma_0 + \mathrm{e}^{\mathrm{i}\varphi}))}{R(\sigma_0 + \mathrm{e}^{\mathrm{i}\varphi}) - z_0} R\mathrm{i}\mathrm{e}^{\mathrm{i}\varphi}\, d\varphi \right)$$

For the second integral on the right-hand side, we have

$$\left| \int_{\frac{\pi}{2}}^{-\frac{\pi}{2}} \frac{f(R(\sigma_0 + \mathrm{e}^{\mathrm{i}\varphi}))}{R(\sigma_0 + \mathrm{e}^{\mathrm{i}\varphi}) - z_0} R\mathrm{i}\mathrm{e}^{\mathrm{i}\varphi}\, d\varphi \right| \leq \int_{\frac{\pi}{2}}^{-\frac{\pi}{2}} \left| \frac{f(R(\sigma_0 + \mathrm{e}^{\mathrm{i}\varphi}))}{R(\sigma_0 + \mathrm{e}^{\mathrm{i}\varphi}) - z_0} R\mathrm{i}\mathrm{e}^{\mathrm{i}\varphi} \right| d\varphi$$

Since $\sup_{z \in U} |zf(z)| < \infty$, we know that $\left| f(R(\sigma_0 + \mathrm{e}^{\mathrm{i}\varphi})) R\mathrm{i}\mathrm{e}^{\mathrm{i}\varphi} \right|$ is bounded for every R and φ. Hence, the second integral disappears as $R \to \infty$. We thus obtain

$$-f(z_0) = \frac{1}{2\pi\mathrm{i}} \lim_{R \to \infty} \int_{-R}^{R} \frac{f(\sigma_0 + \mathrm{i}t)}{\sigma_0 + \mathrm{i}t - z_0} \mathrm{i}\, dt = \frac{1}{2\pi\mathrm{i}} \int_{\gamma} \frac{f(z)}{z - z_0}\, dz.$$

□

Analogously, the residue theorem can be extended to such a line.

A.2 Weak formulation of integral equations

Since the classical formulation of boundary value problems does not lead to satisfactory results about existence and uniqueness of solutions, one can employ the *weak formulation* (also called *variational formulation*). For this formulation, definitions and theory about adequate functions spaces can be found in [Eva98].

In this subsection, we present a small summary with the main results about such formulation.

Consider the problem of finding the function $\psi \in H^{-s}(\Gamma)$ that solves

$$K\phi = g,$$

where $K: H^{-s}(\Gamma) \to H^{s}(\Gamma)$ is an integral operator and $g \in H^{s}(\Gamma)$ a right-hand side function.

The *weak formulation* of the problem is given by

Find $\phi \in H^{-s}(\Gamma)$ such that

$$\int_\Gamma K\phi \cdot v \, d\Gamma_x = \int_\Gamma g \cdot v \, d\Gamma_x \quad \forall v \in H^{-s}(\Gamma). \tag{A.2}$$

We rewrite this using the inner product $(\cdot,\cdot)_{L^2(\Gamma)}$, extended to $H^{-s}(\Gamma)$:

$$(K\phi, v)_{L^2(\Gamma)} = (g, v)_{L^2(\Gamma)} \quad \forall v \in H^{-s}(\Gamma).$$

A weak solution ϕ of this problem, if it is regular enough, is equivalent to a classical solution. We now want to show the existence and uniqueness of such a weak solution.

Definition 11. For $u, v \in H^{-s}(\Gamma)$ we define the *sesquilinear form*

$$\begin{aligned} a: H^{-s}(\Gamma) \times H^{-s}(\Gamma) &\to \mathbb{C} \\ (u, v) &\mapsto a(u, v) := (Ku, v)_{L^2(\Gamma)} \end{aligned}$$

and the *linear form*

$$\begin{aligned} f: H^{-s}(\Gamma) &\to \mathbb{C} \\ v &\mapsto f(v) := (g, v)_{L^2(\Gamma)}. \end{aligned}$$

Definition 12. Let H be a Hilbert space. A sesquilinear form $a: H \times H \to \mathbb{C}$ is called *H-elliptic* if there exist $\gamma > 0$ and $\sigma \in \mathbb{C}$ with $|\sigma| = 1$ such that

$$\mathrm{Re}(\sigma a(w, w)) \geq \gamma \|u\|_H^2, \qquad \forall w \in H.$$

We can now formulate the *Lax-Milgram* theorem [SS11, Chapter 2.1.6].

Theorem 11 (Lax-Milgram)**.** *Let H be a Hilbert space. Let $a: H \times H \to \mathbb{C}$ be a continuous, H-elliptic sesquilinear form, with γ and σ as in Definition 12. Let $f \in H'$ be a linear form. Then, the equation*

$$a(\phi, w) = f(w) \quad \forall w \in H$$

has a unique solution $\phi \in H$. Furthermore, it holds that

$$\|\phi\|_H \leq \frac{1}{\gamma} \|f\|_{H'}.$$

A.3 The Galerkin discretization

As seen in Subsection 3.2, we employ Galerkin discretization. Therefore, we include some theoretical framework, following [Hac92, Chapter 8.1].

Consider a boundary value problem in its variational formulation:

Find $\phi \in H$ such that

$$a(\phi, v) = g(v) \quad \forall v \in H, \tag{A.3}$$

where a is a continuous bilinear or sesquilinear form on $H \times H$ and $g \in H'$.

Its Galerkin discretization is created by replacing the infinite-dimensional space H with a finite-dimensional space H_N:

$$H_N \subset H, \qquad \dim H_N = N < \infty. \tag{A.4}$$

Note that H_N is still a Hilbert space with the same norm $\|\cdot\|_H$, and that a and g are still defined for elements of H_N. Thus, we may pose the problem

Find $\phi_N \in H_N$ such that

$$a(\phi_N, v) = g(v) \quad \forall v \in H_N. \tag{A.5}$$

To find a solution, one needs a basis of H_N. Let $\{b_1, \dots, b_N\}$ be such a basis, i.e. $H_N = \operatorname{span}\{b_1, \dots, b_N\}$. The problem (A.5) is then equivalent to:

Find $\phi_N \in H_N$ such that

$$a(\phi_N, b_i) = g(b_i) \quad \forall i = 1, \dots, N. \tag{A.6}$$

We can write an element $v \in H_N$ as $\mathbf{v} = (v_1, \dots, v_N) \in \mathbb{R}^N$, where $\mathbf{v} = \sum_{i=1}^N v_i b_i$. The problem then becomes a system of linear equations, as the following theorem illustrates.

Theorem 12. *[Hac92, Theorem 8.1.3] For the $N \times N$-matrix $\mathbf{A}$ and the N-vector $\mathbf{g}$ defined by*

$$\mathbf{A}_{ij} := a(b_j, b_i)$$
$$\mathbf{g}_i := g(b_i)$$

for $1 \le i, j \le N$, the problem (A.6) *is equivalent to finding $\boldsymbol{\phi} \in \mathbb{R}^N$ that solves*

$$\mathbf{A}\boldsymbol{\phi} = \mathbf{g}.$$

Corollary 13. *The Galerkin discretization* (A.6) *has a unique solution for each $g \in H'$ if and only if $\mathbf{A}$ is nonsingular.*